Synthesis and characterization of one- and two-dimensional octacyanometalate(V) networks: {[*trans*-$M^{II}(DMF)_4$][*cis*-$M^{II}(DMF)_4]_2[M^V(CN)_8]_2$}$_n$ (M^{II} = Mn, Fe, Ni; M^V = Mo, W)
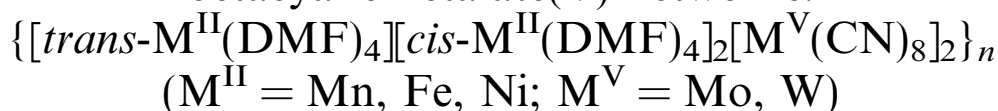
Jeffrey R. Withers [a], Dongfeng Li [a], Jeremy Triplet [a], Chad Ruschman [a], Sean Parkin [a], Guangbin Wang [b], Gordon T. Yee [b], Stephen M. Holmes [a],*

[a] *Department of Chemistry, University of Kentucky, Lexington, KY 40506-0055, USA*
[b] *Virginia Polytechinic Institute and State University, Blacksburg, VA 24061, USA*

Abstract

Treatment of several binary transition metal *p*-toluenesulfonates [$M^{II}(OTs)_2$] with tri(butyl)ammonium octacyanomolybdate(V) or -tungstate(V) in DMF readily affords a series of one- and two-dimensional crystalline octacyanometalate networks of [$M^{II}(DMF)_4]_3[M^V(CN)_8]_2$ (M^V = Mo, W; M^{II} = Mn, **5**, **6**; Ni, **7**, **8**) stoichiometry. Treatment of Fe(OTs)$_2$ with [HBu$_3$N]$_3$[W^V(CN)$_8$] in DMF affords amorphous precipitates while FeCl$_3$ affords crystalline [Fe^{II}(DMF)$_6$]$_2$[W^{IV}(CN)$_8$] (**9**) salts; two-dimensional [Fe^{II}(DMF)$_4$]$_3$[W^V(CN)$_8$]$_2$ (**10**) lattices are obtained from **9** after standing several months. The structures of **5** and **8** contain [*cis*-$M^{II}(DMF)_4(\mu$-NC)$_2$]$^{2+}$ and [*trans*-$M^{II}(DMF)_4(\mu$-NC)$_2$]$^{2+}$ units that are linked via cyanides to three-connected [M^V(CN)$_5(\mu$-CN)$_3$]$^{3-}$ centers, forming a one-dimensional chain of {$M_2^{II}(\mu$-CN)$_4M_2^V$} squares that crystallize in the monoclinic (**5**, $P2_1/n$) and triclinic (**8**, $P\bar{1}$) space groups; **6** ($P2_1/n$) and **10** ($P2_1/c$) crystallize as two-dimensional corrugated sheets containing [*cis*-$M^{II}(DMF)_4(\mu$-NC)$_2$]$^{2+}$, [*trans*-$M^{II}(DMF)_4(\mu$-NC)$_2$]$^{2+}$, and [M^V(CN)$_5(\mu$-CN)$_3$]$^{3-}$ units in a 4:2:6 ratio. Magnetic measurements indicate that **6** is a ferrimagnet (T_N = 8 K) that exhibits frequency-dependent behavior in χ'' that is qualitatively similar to 1- and 2-D lattices reported by Tang and Holmes, respectively; dc magnetic measurements suggest that **5**, **7**, and **8** exhibit incipient magnetic ordering while ac measurements show no frequency-dependent behavior in χ''. Surprisingly, conversion of **5** to **6** in the presence of counterions occurs while heating crystalline samples introduces additional magnetic phases without linkage isomerism; two-dimensional phases containing Mn^{II} centers appear to be the sole product when wet DMF is used as a reaction solvent. The experimental evidence suggests that coordinated DMF ligands are labile and the $M^{II}(\mu$-NC)M^V linkages are susceptible to fragmentation.
© 2007 Elsevier Ltd. All rights reserved.

Keywords: Cyanide networks; Octacyanometalate; Magnetic; Building block approach

1. Introduction

Cyanometalates are versatile building blocks for constructing clusters and extended arrays of metal centers linked via cyanides. Cyanometalates generally form linear M(μ-CN)M′ linkages and are useful building blocks for constructing well-defined materials because they stabilize a variety of transition metal centers and oxidation states and efficiently communicate spin information [1–5]. The magnetic properties of clusters and extended lattices can often be predicted and described via pair-wise exchange interactions that are mediated by the cyanide bridge with the sign of the local exchange interactions predicted by simple molecular orbital symmetry analyses [1–7]. Using building block synthetic strategies, a variety of cyanometalate

---

building blocks are allowed to self-assemble into a common structural archetype, thus allowing for the systematic tuning of the optical and magnetic properties of the resulting reaction products, and accurate magneto-structural correlations to be described; examples include photomagnetic lattices [10–14], room temperature magnets [3–5], and polynuclear complexes [8] and low-dimensional chains that exhibit slow relaxation of the magnetization [9].

The radial extent and diffuseness of second- and third-row transition metal centers present in $[M^n(CN)_8]^{(n-8)}$ anions (Mo, W) are expected to exhibit enhanced π-back-bonding, charge delocalization, and efficient superexchange interactions between metal centers in networks and clusters constructed from M(μ-CN)M′ units [22]. Octacyanometalate anions generally adopt square antiprismatic, bicapped trigonal prismatic, or dodecahedral structures and are capable of forming up to eight cyanide bridges to adjacent metal centers. These factors are expected to afford cyanometalate materials that exhibit markedly different magnetic and optical properties than hexa- and heptacyanometalate derivatives. Octacyanometalates are also attractive building blocks because they undergo facile photoejection of electrons and often form lattices and clusters that exhibit long-lived photo-induced magnetization changes, with several reports indicating that $Cu^{II}/[Mo(CN)_8]^{n-}$ and $Co^{II/III}/[W(CN)_8]^{n-}$ units being the most useful for constructing such photoresponsive networks and clusters [10–14]. While the first examples of lattices containing octacyanometalate anions, $M_2^{II}[Mo^{IV}(CN)_8] \cdot nH_2O$ $(2 \leqslant n \leqslant 9)$ $(M^{II} = Mn,$ Fe, Co, Ni, Cu, and Zn), were reported in 1927 relatively few octacyanometalate clusters and networks have been reported, in comparison to better known hexacyanometalate analogues [15–21].

Recently pentadecanuclear octacyanometalate(V) clusters of $Co^{II}[Co^{II}(MeOH)_3]_8[M^V(CN)_8]_6 \cdot nMeOH$ stoichiometry $(M^V = Mo,$ W) were reported to exhibit slow relaxation of the magnetization that is characteristic of superparamagnetic compounds [22a]. These cyanide-bridged polynuclear complexes are typically prepared in alcoholic media and are often prone to rapid desolvation and aggregation under mild conditions [22]; we rationalized that DMF might be a more suitable donor ligand than alcohols for stabilizing the cluster framework. Methanolic mixtures of these clusters treated with DMF rapidly afforded precipitates while combination of divalent 3d tosylates with octacyanometalate(V) salts in DMF give a series of structurally related one-dimensional chains that are essentially isostructural to "glassy" networks reported by Tang et al. [23,24]. We rationalized that substitution of Mn^{II} for more anisotropic metal centers (e.g. Ni^{II}) might afford magnetic chain analogues that exhibit higher blocking temperatures than Mn^{II} analogues, assuming that efficient superexchange interactions are maintained. Moreover, we rationalized that octacyanometalates may be promising building blocks for constructing polynuclear complexes and lattices that exhibit markedly different and/or enhanced properties (e.g. photomagnetism, magnetism) relative to 3d hexa- and heptacyanometalate analogues [1–5,13–15]. In the present contribution we describe the syntheses, crystallographic, spectroscopic, and magnetic details of several one- and two-dimensional octacyanometalate(V) networks containing a series of paramagnetic 3d transition metal centers.

2. Experimental

2.1. General considerations

All operations were conducted while dark in a vacuum or under an argon atmosphere by using standard Schlenk and drybox techniques. Transfers of solutions containing cyanides were carried out through stainless steel cannulas. The salts Cs(OTs), Mn(OTs)$_2$, Co(OTs)$_2$, Ni(OTs)$_2$, [NBu$_3$H]$_3$[Mo(CN)$_8$], and [NBu$_3$H]$_3$[W(CN)$_8$] were prepared according to modified literature methods [16,17,25–28]. Solvents were distilled under dinitrogen from sodium-benzophenone (diethyl ether) or Mg turnings (methanol and ethanol) and were sparged with argon prior to use. DMF (Baker) was dried over activated Linde 13-X molecular sieves and sparged with argon prior to use. FeCl$_3$ (Cerac), nitric acid (Baker), tributylamine (Aldrich), Celite (Aldrich), and deionized water were used as received.

The IR spectra were recorded as Nujol mulls between KBr plates on a Mattson Galaxy 5200 FTIR instrument. Room temperature powder susceptibility measurements were collected on a Johnson–Matthey magnetic susceptibility balance. Variable temperature and magnetic field measurements were performed at the Frederick Seitz Materials Research Laboratory at the University of Illinois at Urbana-Champaign (U.I.) and Virginia Tech University (V.T.) on Quantum Design MPMS (U.I. and V.T.) and MPMS2 (U.I.) SQUID magnetometers. Diamagnetic corrections were estimated using Pascal's constants [29,30]: $\chi_{dia} = -771.36 \times 10^{-6}$ cm^3 mol^{-1} for **5**, $\chi_{dia} = -771.36 \times 10^{-6}$ cm^3 mol^{-1} for **6**, $\chi_{dia} = -827.36 \times 10^{-6}$ cm^3 mol^{-1} for **5**, $\chi_{dia} = -749.36 \times 10^{-6}$ cm^3 mol^{-1} for **7**, and $\chi_{dia} = -827.36 \times 10^{-6}$ cm^3 mol^{-1} for **8**. Microanalyses were performed by the University of Illinois Microanalysis Laboratory.

2.2. Preparation of complexes and networks

2.2.1. [HBu$_3$N]$_3$[Mo(CN)$_8$] (**1**)

Treatment of aqueous (80 mL) K$_4$[Mo(CN)$_8$] · 2H$_2$O (25.04 g, 50.4 mmol) with concentrated HNO$_3$ (110 mL) over 5 min. affords a brown solution. Subsequent addition of water (200 ml) followed by tributylamine (40 mL, 168 mmol) while stirring affords a pale brown suspension over 10 min; water (1200 mL) was added and the mixture was allowed to stir an additional 30 min. The crude product was isolated by suction filtration and washed with water (3 × 50 mL) followed by Et$_2$O (50 mL). The remaining yellow solid was dissolved into absolute EtOH (250 mL), filtered through Celite, and the pale yellow

filtrate was concentrated under vacuum (60 °C) to *ca.* 100 mL volume. Addition of Et_2O (200 mL) afforded a pale yellow solid that was isolated by suction filtration, washed with Et_2O (2 × 20 mL), and dried under vacuum for 2 h at room temperature (29 °C). Yield: 24.51 g (56.3%). *Anal.* Calc. for $C_{44}H_{84}N_{11}Mo$: C, 61.17; H, 9.83; N, 17.84; Mo, 11.11. Found: C, 61.51; H, 9.70; N, 17.82; Mo, 10.89%. IR (Nujol, cm^{-1}): 3027 (vs, br), 2962 (vs, br), 2935 (vs), 2871 (vs), 2853 (vs), 2798 (vs), 2141 (s), 2114 (w), 1224 (w), 1156 (w), 1107 (w), 1066 (w), 1035 (w), 984 (vw), 931 (w), 902 (vw), 802 (vw), 741 (w), 499 (vw), 487 (vw), 451 (vw).

2.2.2. *[HBu₃N]₃[W(CN)₈] (2)*

Treatment of aqueous (120 mL) $K_4[W(CN)_8] \cdot 2H_2O$ (24.98 g, 42.7 mmol) with concentrated HNO_3 (120 mL) over 3 min. affords a dark purple solution. Subsequent addition of water (200 ml) followed by tributylamine (40 mL, 168 mmol) with stirring gradually affords a pale purple suspension over 10 min; addition of water (750 mL) gradually afforded a pale purple suspension over 30 min. The crude product was isolated via suction filtration and was washed with water (3 × 50 mL) followed by Et_2O (50 mL). The remaining pale purple solid was dissolved into anhydrous EtOH (300 mL) and the mixture was filtered through Celite. The pale purple filtrate was concentrated under vacuum (60 °C) to *ca.* 100 mL volume and Et_2O (100 mL) was added. The precipitated white solid was isolated via suction filtration, washed with Et_2O (3 × 50 mL), and dried under vacuum for 2 h at room temperature (29 °C). Yield: 30.43 g (74.9%). *Anal.* Calc. for $C_{44}H_{84}N_{11}W$: C, 55.52; H, 8.92; N, 16.19. Found: C, 55.57; H, 8.8; N, 16.07%. IR (Nujol, cm^{-1}): 3343 (w), 3321 (w), 3298 (w), 3027 (vs), 2936 (vs), 2871 (vs), 2854 (vs), 2798 (vs), 2748 (s), 2663 (m), 2548 (w), 2144 (m), 2120 (w), 1277 (w), 1224 (w), 1156 (w), 1107 (w), 1066 (w), 1034 (w), 985 (w), 931 (w), 902 (vw), 803 (w), 741 (w), 440 (w).

2.2.3. *Cs₃[Mo(CN)₈] (3)*

Treatment of **1** (5.14 g, 5.95 mmol) in MeOH (50 mL) with methanolic (125 mL) CsOTs (4.94 g, 18.2 mmol) rapidly precipitated a yellow solid. The mixture was allowed to stir for 5 min and the yellow solid was isolated via suction filtration, washed with EtOH (2 × 25 mL) and Et_2O (30 mL), and dried under vacuum for 2 h at room temperature (29 °C). Yield: 4.04 g (91.8%). *Anal.* Calc. for $C_8N_8Cs_3Mo$: C, 13.66; H, 0; N, 15.94; Cs, 56.73; Mo, 13.65. Found: C, 13.72; H, 0; N, 15.31; Cs, 55.98; Mo, 13.22%. IR (Nujol, cm^{-1}): 3615 (w), 3480 (w, br), 3348 (w), 3321 (w), 3298 (w), 2143 (vs), 2135 (s, sh), 2114 (w), 1606 (vw), 505 (w), 471 (w).

2.2.4. *Cs₃[W(CN)₈] (4)*

Treatment of CsOTs (6.11 g, 22.5 mmol) in MeOH (50 mL) with methanolic **2** (7.24 g, 7.61 mmol) rapidly affords a pale yellow suspension. The mixture was allowed

to stir for 15 min. and subsequently filtered via suction filtration. The yellow precipitate was washed with EtOH (2 × 10 mL) and Et_2O (2 × 15 mL) and dried for 2 h under vacuum at room temperature (30 °C). Yield: 5.18 g (86.0%). *Anal.* Calc. for $C_8H_8N_8Cs_3W$: C, 12.14; H, 0; N, 14.16; Cs, 50.43; W, 23.25. Found: C, 12.31; H, 0.03; N, 13.6; Cs, 48.57; W, 20.19%. IR (Nujol, cm^{-1}): 3603 (w), 3532 (w), 2144 (m), 2131 (m), 1619 (w), 446 (w), 420 (w).

2.2.5. *{[trans-Mnᴵᴵ(DMF)₄][cis-Mnᴵᴵ(DMF)₄]₂- [Wⱽ(CN)₈]₂}ₙ (5)*

Treatment of a DMF (20 mL) solution of $Mn(OTs)_2$ (1.25 g, 3.15 mmol) with **2** (1.98 g, 2.08 mmol) in DMF (20 mL) afforded an amber solution that was allowed to stand for 4 d at room temperature (20 °C). The brown crystals were isolated via filtration, washed with DMF (2 × 5 mL) and Et_2O (3 × 5 mL), and dried under vacuum for 2 min at room temperature (20 °C). Yield: 1.25 g, (65.8%). *Anal.* Calc. for $C_{52}H_{84}N_{28}O_{12}Mn_3W_2$: C, 34.21; H, 4.64; N, 21.48; Mn, 9.03; W, 20.14. Found: C, 34.02; H, 4.11; N, 20.87%. IR (Nujol, cm^{-1}): 3144 (s), 3062 (s), 2157 (vs), 2130 (m, sh), 2114 (w), 1645 (vs), 1560 (s), 1540 (s), 1496 (vs), 1454 (vs), 1421 (vs), 1251 (vs), 1154 (m), 1110 (vs), 1062 (s), 1016 (m), 865 (m), 678 (s), 675 (s), 439 (s), 421 (s).

2.2.6. *{[trans-Mnᴵᴵ(DMF)₄][cis-Mnᴵᴵ(DMF)₄]₂- [Wⱽ(CN)₈]₂}ₙ (6)*

Treatment of a DMF (20 mL) solution of $Mn(OTs)_2$ (1.17 g, 2.94 mmol) with **2** (2.59 g, 2.72 mmol) in DMF (20 mL) afforded an amber solution that was allowed to stand for 4 d at room temperature (28 °C). The brown crystals were isolated by filtration, washed with DMF (2 × 5 mL) and Et_2O (3 × 5 mL), and dried under vacuum for 2 min at room temperature (28 °C). Yield: 1.51 g, (84.4%). *Anal.* Calc. for $C_{52}H_{84}N_{28}O_{12}Mn_3W_2$: C, 34.21; H, 4.64; N, 21.48; Mn, 9.03; W, 20.14. Found: C, 34.05; H, 4.31; N, 20.83%. IR (Nujol, cm^{-1}): 3143 (s), 3060 (s), 2156 (vs), 2129 (m, sh), 2113 (w, sh), 2029 (w), 2016 (w, sh), 1645 (vs), 1559 (s), 1540 (s), 1496 (vs), 1456 (vs), 1420, (vs), 1252 (vs), 1152 (m), 1110 (vs), 1062 (s), 1017 (m), 865 (m), 678 (s), 674 (s), 439 (s), 421 (s), and 403 (s).

2.2.7. *{[trans-Niᴵᴵ(DMF)₄][cis-Niᴵᴵ(DMF)₄]₂- [Moⱽ(CN)₈]₂}ₙ (7)*

Treatment of a DMF (20 mL) solution of $Ni(OTs)_2$ (1.25 g, 3.12 mmol) with **1** (1.95 g, 2.25 mmol) in DMF (20 mL) afforded a lime-green solution that was allowed to stand for 4 d at room temperature (26 °C). The pale green crystals were isolated by filtration, washed with DMF (2 × 5 mL) and Et_2O (3 × 5 mL), and dried under vacuum for 2 min. at room temperature (26 °C). Yield: 1.07 g, (62.1%). *Anal.* Calc. for $C_{52}H_{84}N_{28}O_{12}Mo_2Ni_3$: C, 37.58; H, 5.09; N, 23.60; Ni, 23.61; Mo, 11.55. Found: C, 36.98; H, 4.85; N, 22.91%. IR (Nujol, cm^{-1}): 3140 (m), 3055 (m, sh), 2193 (m, sh), 2183 (m), 2138 (w), 1672 (vs), 1643 (vs), 1548 (w), 1499 (s), 1456 (vs), 1439 (vs), 1422

(vs), 1378 (vs), 1254 (s), 1151 (m), 1114 (vs), 1096 (s), 1063 (s), 1011 (m), 869 (w), 685 (s), 658 (m), 520 (w), 487 (m).

2.2.8. {[trans-Ni^{II}(DMF)$_4$][cis-Ni^{II}(DMF)$_4$]$_2$-[W^V(CN)$_8$]$_2$}$_n$ (8)

Treatment of a DMF (20 mL) solution of Ni(OTs)$_2$ (1.25 g, 3.12 mmol) with **2** (2.16 g, 2.27 mmol) in DMF (20 mL) afforded a lime-green solution that was allowed to stand for 4 d at room temperature (26 °C). The pale green crystals were isolated by filtration, washed with DMF (2 × 5 mL) and Et$_2$O (3 × 5 mL), and dried under vacuum for 2 min at room temperature (26 °C). Yield: 1.21 g, (63.3%). *Anal.* Calc. for C$_{52}$H$_{84}$N$_{28}$O$_{12}$Ni$_3$W$_2$: C, 33.99; H, 4.61; N, 21.35; Ni, 9.58; W, 20.01. Found: C, 33.54; H, 3.96; N, 20.54%. IR (Nujol, cm^{-1}): 3142 (w), 3052 (m, sh), 2186 (m), 2170 (m, sh), 2137 (w), 1671 (vs), 1643 (vs), 1548 (m), 1499 (s), 1454 (vs, sh), 1440 (vs), 1422 (vs), 1378 (vs), 1255 (s), 1150 (m, sh), 1114 (vs), 1096 (s, sh), 1063 (s), 1017 (m), 869 (w), 816 (w, sh), 693 (s, sh), 684 (s), 658 (w), 478 (w), 454 (m).

2.2.9. [Fe^{II}(DMF)$_6$]$_2$[W^{IV}(CN)$_8$] (9)

Treatment of a DMF (15 mL) solution of FeCl$_3$ (0.17 g, 1.05 mmol) with **2** (1.01 g, 1.06 mmol) in DMF (15 mL) afforded a dark orange solution; after 3 d (20 °C) Et$_2$O (20 mL) was layered on top of the yellow mixture forming yellow crystals within 1 week. The crystals were isolated via filtration, washed with DMF (3 × 5 mL) and Et$_2$O (3 × 5 mL), and dried under vacuum for 16 h at room temperature (20 °C). Yield: 0.86 g (60.9%). *Anal.* Calc. for C$_{44}$H$_{84}$N$_{20}$O$_{12}$Fe$_2$W: C, 38.24; H, 6.14; N, 20.28. Found:

C, 37.88; H, 5.75; N, 19.69%. IR (Nujol, cm^{-1}): 3142 (w), 3053 (vs), 2923 (vs), 2854 (vs), 2181 (w), 2164 (w), 2151 (w), 2121 (w), 1683 (vs, sh), 1671 (vs, sh), 1645 (vs), 1496 (m), 1455 (s), 1439 (s), 1378 (vs), 1254 (m), 1152 (w), 1117 (s), 1094 (m), 1064 (m), 1019 (m), 685 (m), 671 (m, sh), 661 (w), 447 (m), 403 (s). μ_{eff} (μ_B) = 6.79. Upon standing several months DMF/Et$_2$O mixtures of **9** afford small quantities of {[trans-Fe^{II}(DMF)$_4$][cis-Fe^{II}(DMF)$_4$]$_2$-[W^V(CN)$_8$]$_2$}$_n$ (**10**) as brown crystals. IR (Nujol, cm^{-1}): 3144 (m), 3056 (m), 2280 (w, sh), 2155 (m, sh), 2145 (m), 2127 (m), 2116 (m), 2029 (w), 1658 (vs), 1642 (vs), 1495 (s), 1456 (vs), 1439 (vs), 1253 (s), 1150 (w), 1115 (vs), 1064 (s), 866 (w), 805 (w), 683 (vs), 441 (m), 417 (s).

2.3. Structure determinations and refinements

Crystals of **5–8** were grown from DMF solutions of either Mn(OTs)$_2$ (**5, 6**), Ni(OTs)$_2$ (**7, 8**), or FeCl$_3$ (**9, 10**) treated with **1** or **2**. X-ray diffraction data were collected at 90.0(2) K on a Nonius kappaCCD diffractometer from irregular shaped crystals, mounted in Paratone-N oil on glass fibers. Initial cell parameters were obtained (DENZO) [31] from ten 1° frames and were refined via a least-squares scheme using all data-collection frames (SCALEPACK) [31]. Lorentz/polarization corrections were applied during data reduction. The structures were solved by direct methods (SHELXS97) [32] and completed by difference Fourier methods (SHELXL97) [32]. Refinement was performed against F^2 by weighted full-matrix least-squares (SHELXL97) [32] and empirical absorption corrections (either SCALEPACK [31] or SADABS [32]) were applied. Hydrogen atoms were found in difference maps and subsequently placed at calculated posi-

Table 1
Crystallographic data for {[*trans*-Mn^{II}(DMF)$_4$][*cis*-Mn^{II}(DMF)$_4$]$_2$[W^V(CN)$_8$]$_2$}$_n$ (**5**), {[*trans*-Mn^{II}(DMF)$_4$][*cis*-Mn^{II}(DMF)$_4$]$_2$[W^V(CN)$_8$]$_2$}$_n$ (**6**), {[*trans*-Ni^{II}(DMF)$_4$][*cis*-Ni^{II}(DMF)$_4$]$_2$[W^V(CN)$_8$]$_2$}$_n$ (**8**), [Fe^{II}(DMF)$_6$]$_2$[W^{IV}(CN)$_8$] (**9**), and {[*trans*-Fe^{II}(DMF)$_4$][*cis*-Fe^{II}(DMF)$_4$]$_2$[W^V(CN)$_8$]$_2$}$_n$ (**10**)

	5	6	8	9	10
Chemical formula	C$_{52}$H$_{84}$Mn$_3$N$_{28}$O$_{12}$W$_2$	C$_{52}$H$_{84}$Mn$_3$N$_{28}$O$_{12}$W$_2$	C$_{52}$H$_{84}$N$_{28}$Ni$_3$O$_{12}$W$_2$	C$_{44}$H$_{84}$Fe$_2$N$_{20}$O$_{12}$W	C$_{52}$H$_{84}$N$_{28}$Fe$_3$O$_{12}$W$_2$
Formula weight	1826.00	1826.00	1837.30	1380.82	1828.72
Temperature (K)	90.0(2)	90.0(2)	90.0(2)	90.0(2)	90.0(2)
λ (Å)	0.71073	0.71073	0.71073	0.71073	0.71073
Crystal size (mm)	0.25 × 0.20 × 0.20	0.28 × 0.22 × 0.20	0.15 × 0.15 × 0.15	0.20 × 0.20 × 0.15	0.38 × 0.32 × 0.25
Space group	P2$_1$/n	P2$_1$/n	P$\bar{1}$	P2$_1$/c	P2$_1$/c
Crystal system	monoclinic	monoclinic	triclinic	monoclinic	monoclinic
a (Å)	17.6370(2)	11.0050(1)	11.5800(1)	9.9660(1)	11.0030(1)
b (Å)	12.0850(1)	20.6320(2)	12.5510(1)	19.3100(2)	20.5090(3)
c (Å)	18.5330(2)	16.7420(2)	13.4950(1)	19.4650(3)	18.0580(3)
V (Å^3)	3740.81(7)	3725.69(7)	1834.63(3)	3698.94(8)	3695.28(9)
α (°)			86.6240(4)		
β (°)	108.7380(5)	101.4510(5)	73.8650(4)	99.0830(6)	114.9301(5)
γ (°)			76.8430(4)		
ρ (g cm^{-3})	1.621	1.796	1.663	1.592	1.644
Z	4	4	2	4	2
μ (mm^{-1})	3.628	3.503	3.952	3.556	3.749
Final R indices [I > 2σ(I)][a]	R$_1$ = 0.0203, wR$_2$ = 0.0401	R$_1$ = 0.0177, wR$_2$ = 0.0359	R$_1$ = 0.0224, wR$_2$ = 0.0546	R$_1$ = 0.0240, wR$_2$ = 0.0520	R$_1$ = 0.0349, wR$_2$ = 0.0615
R indices (for all data)	R$_1$ = 0.0288, wR$_2$ = 0.0419	R$_1$ = 0.0236, wR$_2$ = 0.0373	R$_1$ = 0.0261, wR$_2$ = 0.0566	R$_1$ = 0.0305, wR$_2$ = 0.0541	R$_1$ = 0.0657, wR$_2$ = 0.0693

[a] $R = \sigma\|F_o| - |F_o\|/\sum|F_o|$. $wR = \left[\left(\sum w(|F_o| - |F_c|)^2 / \sum wF_o^2\right)\right]^{1/2}$.

tions using suitable riding models with isotropic displacement parameters derived from their carrier atoms. Non-hydrogen atoms were refined with anisotropic displacement parameters. Atomic scattering factors were taken from the International Tables for Crystallography vol. C.3 [33]. Crystal data, relevant details of the structure determinations, and selected geometrical parameters are provided in Tables 1–3.

Table 2
Selected bond distances (Å) for $\{[trans\text{-}Mn^{II}(DMF)_4][cis\text{-}Mn^{II}(DMF)_4]_2[W^V(CN)_8]_2\}_n$ (5), $\{[trans\text{-}Mn^{II}(DMF)_4][cis\text{-}Mn^{II}(DMF)_4]_2[W^V(CN)_8]_2\}_n$ (6), $\{[trans\text{-}Ni^{II}(DMF)_4][cis\text{-}Ni^{II}(DMF)_4]_2[W^V(CN)_8]_2\}_n$ (8), $[Fe^{II}(DMF)_6]_2[W^{IV}(CN)_8]$ (9), and $\{[trans\text{-}Fe^{II}(DMF)_4][cis\text{-}Fe^{II}(DMF)_4]_2[W^V(CN)_8]_2\}_n$ (10)

5		6		8		9		10	
W1–C1	2.184(2)	W1–C1	2.161(2)	W1–C1	2.167(3)	W1–C1	2.168(3)	W1–C1	2.155(6)
W1–C2	2.168(2)	W1–C2	2.170(3)	W1–C2	2.175(3)	W1–C2	2.181(3)	W1–C2	2.177(6)
W1–C3	2.173(2)	W1–C3	2.172(3)	W1–C3	2.161(3)	W1–C3	2.172(3)	W1–C3	2.155(6)
W1–C4	2.168(2)	W1–C4	2.160(3)	W1–C4	2.161(3)	W1–C4	2.186(3)	W1–C4	2.156(6)
W1–C5	2.162(2)	W1–C5	2.169(2)	W1–C5	2.159(3)	W1–C5	2.167(3)	W1–C5	2.174(5)
W1–C6	2.171(2)	W1–C6	2.177(3)	W1–C6	2.168(3)	W1–C6	2.179(3)	W1–C6	2.177(5)
W1–C7	2.162(2)	W1–C7	2.158(3)	W1–C7	2.169(3)	W1–C7	2.172(3)	W1–C7	2.175(6)
W1–C8	2.157(2)	W1–C8	2.179(3)	W1–C8	2.167(3)	W1–C8	2.168(3)	W1–C8	2.172(6)
C1–N1	1.146(3)	C1–N1	1.141(3)	C1–N1	1.146(4)	C1–N1	1.139(4)	C1–N1	1.160(6)
C2–N2	1.149(3)	C2–N2	1.142(3)	C2–N2	1.149(4)	C2–N2	1.147(4)	Fe1–N1	2.137(5)
C6–N6	1.147(3)	C4–N4	1.153(3)	C6–N6	1.141(4)	C3–N3	1.145(4)	Fe1–N4A	2.170(4)
Mn1–N1	2.261(2)	Mn1–N1	2.245(2)	Ni1–N1	2.044(3)	Fe1–O1A	1.975(2)	Fe1–O1	2.108(3)
Mn1–O1A	2.162(2)	Mn1–O1	2.164(2)	Ni1–O1A	2.063(2)	Fe1–O1B	1.984(2)	Fe1–O2	2.148(3)
Mn1–O1AA	2.162(2)	Mn1–O2	2.172(2)	Ni1–O1AA	2.063(2)	Fe1–O1C	2.006(2)	Fe1–O3	2.155(3)
Mn1–O1B	2.167(2)	Mn1–O3	2.158(2)	Ni1–O1B	2.057(2)	Fe2–O1D	2.008(2)	Fe1–O4	2.100(4)
Mn1–O1BA	2.168(2)	Mn1–O4	2.176(2)	Ni1–O1BA	2.057(2)	Fe2–O1E	2.000(2)	Fe2–O5	2.095(3)
Mn2–O1C	2.174(2)	Mn2–O5	2.10(1)	Ni2–O1C	2.057(2)	Fe2–O1F	2.196(2)	Fe2–O6	2.123(4)
Mn2–O1D	2.134(2)	Mn2–O6	2.158(2)	Ni2–O1D	2.047(2)			Fe2–N7	2.154(4)
Mn2–O1E	2.126(2)	Mn2–N2	2.232(2)	Ni2–O1E	2.070(2)			Fe1···Fe1A	8.576(5)
Mn2–O1F	2.172(2)	Mn1–N4A	2.217(2)	Ni2–O1F	2.064(2)			W1···W1B	10.809(5)
Mn2–N6	2.258(2)	Mn1···Mn1E	8.535(3)	Ni2–N6	2.073(5)			W1B···W1BA	23.462(5)
N2–Mn2	2.245(2)	Mn2···Mn2A	18.118(3)	N2–Ni2	2.064(5)			Fe2···Fe2A	18.058(5)
Mn2···Mn2B	6.590(3)	W1···W1A	10.925(3)	W1···Ni1	5.313(4)				
W1···W1B	8.644(3)	W1···Mn1	5.472(3)	W1···Ni2	5.267(4)				
W1···Mn1	5.562(3)	W1A···W1AB	23.629(3)	W1···W1A	8.394(4)				
W1···Mn2	5.452(3)			Ni2···Ni2A	6.382(4)				

Table 3
Selected bond angles (°) for $\{[trans\text{-}Mn^{II}(DMF)_4][cis\text{-}Mn^{II}(DMF)_4]_2[W^V(CN)_8]_2\}_n$ (5), $\{[trans\text{-}Mn^{II}(DMF)_4][cis\text{-}Mn^{II}(DMF)_4]_2[W^V(CN)_8]_2\}_n$ (6), $\{[trans\text{-}Ni^{II}(DMF)_4][cis\text{-}Ni^{II}(DMF)_4]_2[W^V(CN)_8]_2\}_n$ (8), $[Fe^{II}(DMF)_6]_2[W^{IV}(CN)_8]$ (9), and $\{[trans\text{-}Fe^{II}(DMF)_4][cis\text{-}Fe^{II}(DMF)_4]_2[W^V(CN)_8]_2\}_n$ (10)

(5)		(6)		(8)		(9)		(10)	
C1–W1–C2	131.81(8)	C1–W1–C2	87.48(9)	C1–W1–C2	130.8(1)	C1–W1–C2	70.9(2)	C1–W1–C2	76.1(2)
C1–W1–C3	72.38(8)	C1–W1–C3	79.31(9)	C1–W1–C3	72.0(1)	C1–W1–C3	94.9(1)	C1–W1–C3	90.2(2)
C1–W1–C4	75.93(8)	C1–W1–C4	148.13(9)	C1–W1–C4	73.6(1)	C1–W1–C4	142.8(1)	C1–W1–C4	148.0(2)
C1–W1–C5	142.88(8)	C1–W1–C5	141.34(9)	C1–W1–C5	140.1(1)	C1–W1–C5	145.3(1)	C1–W1–C5	141.0(2)
C1–W1–C6	130.53(8)	C1–W1–C6	76.40(9)	C1–W1–C6	137.4(1)	C1–W1–C6	76.4(1)	C1–W1–C6	70.5(2)
C1–W1–C7	71.47(8)	C1–W1–C7	96.62(9)	C1–W1–C7	73.0(1)	C1–W1–C7	75.9(1)	C1–W1–C7	102.5(2)
C1–W1–C8	76.69(8)	C1–W1–C8	70.60(9)	C1–W1–C8	74.5(1)	C1–W1–C8	94.1(1)	C1–W1–C8	77.0(2)
N1–C1–W1	178.7(2)	N1–C1–W1	176.2(2)	N1–C1–W1	176.9(3)	N1–C1–W1	179.3(3)	N1–C1–W1	177.1(5)
N2–C2–W1	175.7(2)	N2–C2–W1	179.1(2)	N2–C2–W1	176.0(3)	N2–C2–W1	178.9(3)	N4–C4–W1	174.9(4)
N6–C6–W1	179.1(2)	N4–C4–W1	178.3(2)	N6–C6–W1	175.8(3)	N3–C3–W1	178.7(3)	N7–C7–W1	179.7(5)
C2–W1–C6	70.64(8)	C2–W1–C6	140.01(9)	C2–W1–C6	71.6(1)	O1A–Fe1–O1B	93.05(9)	C4–W1–C7	88.2(2)
Mn1–N1–C1	168.5(2)	Mn1–N1–C1	157.7(2)	Ni1–N1–C1	167.0(3)	O1A–Fe1–O1C	91.8(1)	Fe1–N1–C1	163.6(4)
N1–Mn1–O1A	92.24(6)	N1–Mn1–O1	91.25(7)	N1–Ni1–O1A	92.1(1)	O1D–Fe2–O1E	87.81(9)	N1–Fe1–O1	95.4(2)
N1–Mn1–O1AA	87.76(6)	N1–Mn1–O2	83.62(7)	N1–Ni1–O1AA	87.9(1)	O1D–Fe2–O1F	87.49(9)	N1–Fe1–O2	173.2(2)
N1–Mn1–O1B	85.90(6)	N1–Mn1–O3	173.42(7)	N1–Ni1–O1B	91.9(1)			N1–Fe1–O3	87.0(2)
N1–Mn1–O1BA	94.10(6)	N1–Mn1–O4	169.66(6)	N1–Ni1–O1BA	88.1(1)			N1–Fe1–O4	88.6(2)
Mn2–N2–C2	159.5(2)	Mn2–N2–C2	160.2(2)	Ni2–N2–C2	157.4(2)			N1–Fe1–N4A	97.5(2)
Mn2–N6A–C6A	152.7(2)	Mn1–N4–C4	164.2(2)	Ni2–N6A–C6A	93.7(1)			Fe2–N7–C7	161.9(4)
N2–Mn2–O1C	92.28(6)	N2–Mn2–O5	95.9(3)	N2–Ni2–O1C	88.58(9)			N7–Fe2–O5	88.3(1)
N2–Mn2–O1D	87.32(6)	N2–Mn2–O6	92.78(7)	N2–Ni2–O1D	93.97(9)			N7–Fe2–O5B	91.7(1)
N2–Mn2–O1E	178.93(6)			N2–Ni2–O1E	177.65(9)			N7–Fe2–O6	85.0(2)
N2–Mn2–O1F	89.48(6)			N2–Ni2–O1F	88.99(9)			N7–Fe2–O6B	95.1(2)
N2–Mn2–N6A	91.34(7)			N2–Ni2–N6A	93.7(1)				

3. Results and discussion

3.1. Syntheses and infrared characterization

We had initially anticipated that a series of isostructural clusters of $M^{II}[M^{II}(DMF)_3]_8[M^V(CN)_8]_6 \cdot n$DMF stoichiometry, would be obtained upon treatment of binary transition metal p-toluenesulfonates with tri(butyl)ammonium octacyanometalates in DMF at room temperature. Instead of clusters several networks are obtained, suggesting that solvent choice is a critical factor in preparing octacyanometalate materials. Treatment of several binary transition metal p-toluenesulfonates $[M^{II}(OTs)_2]$ with **1** or **2** in DMF readily affords one- and two-dimensional crystalline octacyanometalate networks of $[M^{II}(DMF)_4]_3[M^V(CN)_8]_2$ ($M^V = $ Mo, W; $M^{II} = $ Mn, **5**, **6**; Ni, **7**, **8**) stoichiometry [23,24]; Attempts to prepare iron(II) analogues from $Fe^{II}(OTs)_2$ salts consistently afford intractable amorphous precipitates while iron(III) chloride initially affords a trimetallic salt $[Fe^{II}(DMF)_6]_2[W^{IV}(CN)_8]$ (**9**), and small crystalline quantities of $\{[Fe^{II}(DMF)_6]_3[W^V(CN)_8]_2\}_n$ (**10**) after standing for several months.

The infrared spectra of **1–4** exhibit several high-energy cyano stretching absorptions (v_{CN}) that are characteristic of octacyanometalate(V) salts. The v_{CN} stretches are found between 2114 and 2144 cm^{-1} for tributylammonium salts (**1** and **2**) while cesium analogues range from 2131 to 2143 cm^{-1} (**3** and **4**). The energies of the v_{CN} absorptions fall within expected value ranges and elemental analysis data support their formulation as octacyanometalate(V) salts [20,45].

Likewise, compounds **5–8** and **10** exhibit several intense, high-energy v_{CN} absorptions in their infrared spectra. The highest energy cyano stretching absorptions are shifted to higher energies in comparison to those seen in **1** and **2**, and appear to scale as a function of divalent metal center electronegativity, consistent with the presence of $M^{II}(\mu\text{-NC})M^V$ units in **5–8**. Generally, the v_{CN} absorptions range from 2129 to 2193 cm^{-1} suggesting that both bridging and terminal cyanides are present. The Mn^{II} analogues (**5** and **6**) exhibit low-energy v_{CN} absorptions near 2156 cm^{-1}, while the Ni^{II} derivatives (**7**, **8**) have absorptions that are shifted to much higher energies (2183–2193 cm^{-1}), suggesting that these modes are due to bridging cyanides; this trend is generally consistent with increasing π backbonding and decreasing depopulation of the cyanide 5σ orbital within the $M^{II}(\mu\text{-NC})M^V$ unit progressing from Ni^{II} to Mn^{II} [20,36–45]. Additional v_{CN} stretches are also present at lower energies in the infrared spectra of **5–8** and **10** being close in energy to those found for **1** and **2**; we tentatively assign these as terminal cyanide v_{CN} absorptions. For **10**, v_{CN} stretching absorptions are found at 2155, 2127, and 2116 cm^{-1}, suggesting that bridging and terminal cyanides are also present. Assuming that kinematic effects [46] are absent in **5–8** and **10** we conclude that the bridging and terminal cyano stretching absorptions are those

between ca. 2156–2193 cm^{-1} and 2129–2138 cm^{-1}, respectively [10b,18a,20–22,36–47].

For **9**, the infrared spectrum exhibits cyano stretching absorptions that are comparable in energy to ionic octacyanotungstate(IV) salts that are absent of μ-CN linkages. Octacyanometalate(IV) compounds generally exhibit v_{CN} stretches that range from 2060 to 2160 cm^{-1} and 2085 to 2141 cm^{-1} for terminal and bridging cyanides, respectively [20,34–47]. In the infrared spectrum of **9** three medium intensity cyano stretching absorptions [2145, 2127, 2116 cm^{-1}] are found, in addition to a weak v_{CN} at 2029 cm^{-1}, suggesting that $[M^{IV}(CN)_8]^{4-}$ centers are present. The energy of the v_{CN} absorptions found for **9** are markedly different than those observed for $K_4[W^{IV}(CN)_8] \cdot 2H_2O$ (2125, 2095, and 2056 cm^{-1}) and bi- and trimetallic clusters of $[M^{II}(en)_3][cis\text{-}M^{II}(en)_2(OH_2)(\mu\text{-NC})M^{IV}(CN)_7] \cdot 2H_2O$ and $[M^{II}(en)_2(OH_2)]_2[(\mu\text{-NC})_2M^{IV}(CN)_6] \cdot 6H_2O$ stoichiometry (2142–2062 cm^{-1}) [20x,44].

3.2. Crystallographic studies: one-dimensional chains

Compounds **5** and **8** crystallize in the monoclinic ($P2_1/n$) and triclinic ($P\bar{1}$) space groups, respectively (Table 1). The neutral networks consist of an alternating array of distorted $\{[cis\text{-}M^{II}(DMF)_4(\mu\text{-NC})_2M^V(CN)_5(\mu\text{-CN})]_2\}^{2-}$ squares that are linked via bridging cyanides to adjacent $[trans\text{-}(\mu\text{-CN})M^{II}(DMF)_4(\mu\text{-NC})]^{2+}$ units, leaving five terminal cyanides per three-connected $[W^V(CN)_8]^{3-}$ center. The one-dimensional $\{[trans\text{-}M^{II}(DMF)_4][cis\text{-}M^{II}(DMF)_4]_2[(\mu\text{-NC})_3W^V(CN)_5]_2\}_n$ chains (Figs. 1 and 2) are separated by coordinated DMF ligands and have closest $M^{II} \cdots M^{II}$ interchain contacts of ca. 7.61(3) and 8.43(3) Å for **5** and **8**, respectively [23,24]; this structural motif has been previously reported by Shore, Tang, and Colacio for "expanded Prussian blues" and a few octacyanometalate(V) lattices [15,20–24,48].

For the octacyanotungstate(V) centers the W–C bond lengths differ slightly, ranging from 2.157(2) to 2.184(2) Å and 2.159(3) to 2.169(3) Å for **5** and **8**, respectively (Table 2). For **5**, the C–W–C bond angles range from 70.64(8) to 142.88(8)° while the W–C–N bond angles are nearly linear, ranging from 175.7(2) to 179.1(2)° (Table 3). For **8**, the C–W–C bond angles range from 72.0(1) to 140.1(1)° and nearly linear W–C–N bond angles are again found (Table 3); the bridging cyanide C2–W1–C6 and C1–W1–C2 angles are 70.64(8) and 131.81(8)° for **5** and 71.6(1) and 130.8(1)° for **8**. The coordination geometries of the $[W^V(CN)_8]^{3-}$ centers are best described as distorted square antiprismatic (Fig. 1) [20–24,34–47].

The $\{M_2^V(\mu\text{-CN})_4M_2^{II}\}$ fragments in each chain appear to distort as a function of the divalent center present. The M^{II}–N bond distances present in the $[cis\text{-}M^{II}(DMF)_4(\mu\text{-NC})_2]^{2+}$ units contained within the $\{M_2^V(\mu\text{-CN})_4M_2^{II}\}$ fragments appear to scale as a function of divalent metal center ionic radii, with the longest M^{II}–N distances found in **5** [2.245(2) and 2.258(2) Å], while those in **8** [2.064(3) and 2.073(3) Å] are shorter. The M^{II}–
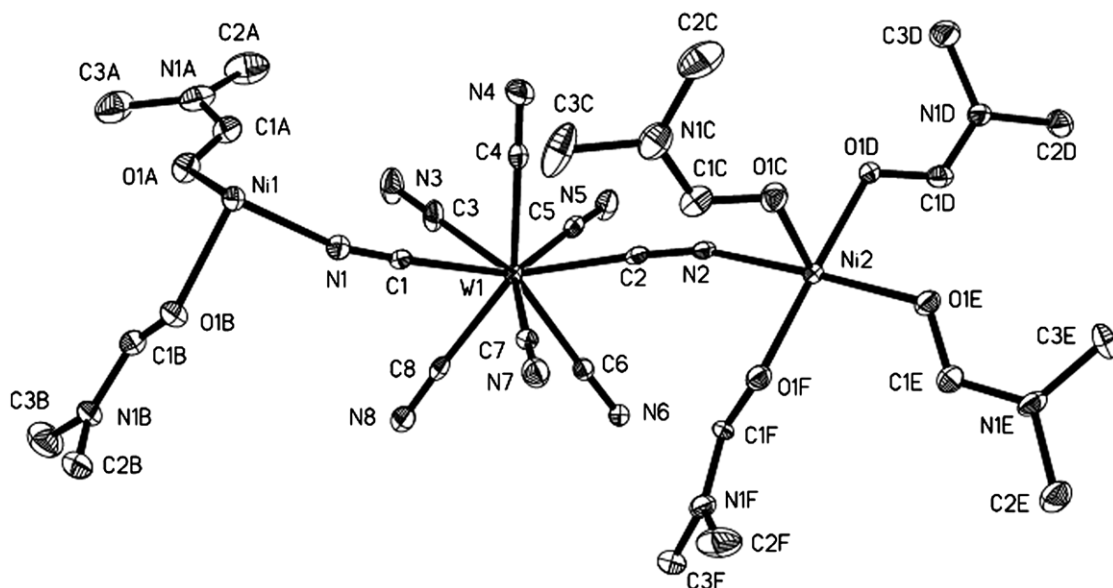
Fig. 1. Asymmetric unit of **8**. Thermal ellipsoids are at the 50% level and all hydrogen atoms are removed for clarity.
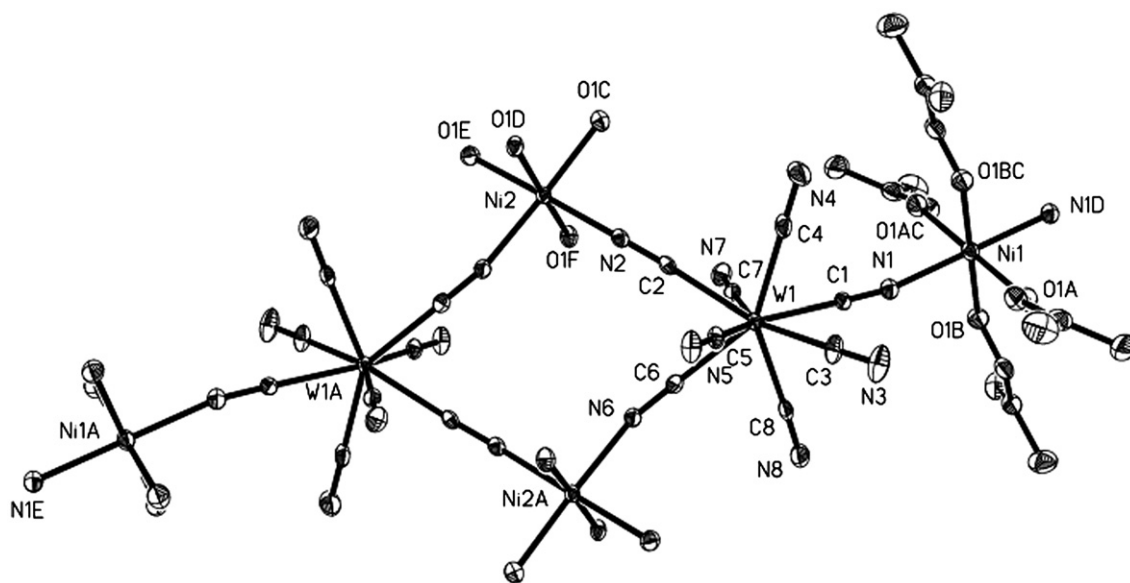

Fig. 2. X-ray structure of **8** illustrating the one-dimensional chain of squares motif present. Thermal ellipsoids are at the 50% probability level and all hydrogen atoms and selected carbon and nitrogen atoms are removed for clarity.

O_{DMF} bond distances range from 2.156(2) to 2.172(2) Å and 2.047(2) to 2.064(2) Å for **5** and **8**, with no discernable trends regarding their relationship to the coordinated cyanides (Table 2). The twisting of the imbedded tetranuclear fragments can be described via the distance of the metal centers from a mean plane defined the atoms present within the $\{M_2^V(\mu\text{-}CN)_4M_2^{II}\}$ fragment; the tungsten and manganese centers in **5** are *ca.* ±0.27(1) and ±0.23(2) Å from this plane, while the tungsten and nickel centers in **8** are located at slightly larger and smaller distances [*ca.* ±0.41(2) and ±0.05(4) Å], respectively. As a final means of comparison, the $M^{II}\cdots M^{II}$ and $W\cdots W$ contacts are slightly larger in **5** [6.59(2) and 8.64(2) Å], while those in **8** [6.39(3) and

8.39(2) Å] are smaller, suggesting that the $\{M_2^V(\mu\text{-}CN)_4M_2^{II}\}$ fragment size depends on the divalent metal centers present.

Significant distortion of the $\{M_2^V(\mu\text{-}CN)_4M_2^{II}\}$ fragments is also apparent in the $N–M^{II}–N$ and $N–M^{II}–O$ bond angles present in **5** and **8**. The smallest $N–M^{II}–N$ and largest $N–M^{II}–O$ bond angles are found for **5**, suggesting that $M^{II}–N$ bond distances are related to the electronegativity and radius of the divalent centers present, affording highly distorted $\{M_2^V(\mu\text{-}CN)_4M_2^{II}\}$ fragments within the one-dimensional chains (Table 3). The $N–M^{II}–N$ bond angles are more acute in **5** [91.34(7)°] in comparison to those seen for **8** [93.7(1)°], while larger N2–M2–O1C and N2–M2–

O1E bond angles are found for **5** [92.28(6) and 178.93(6)°]. Consistent with expected periodic trends compound **8** has slightly smaller N2–M2–O1C and N2–M2–O1E angles [88.99(9) and 177.65(9)°] in comparison to those seen in **5**.

The remaining [*trans*-M^{II}(μ-NC)$_2$(DMF)$_4$]$^{2+}$ units in **5** and **8** have M^{II}–N and M^{II}–O bond distances that are comparable to those seen in the $\{M_2^V(\mu\text{-CN})_4M_2^{II}\}$ units. The average M^{II}–N and M^{II}–O bond distances are 2.252(2) and 2.165(2) Å for **5**, while **8** exhibits smaller distances [2.069(3) and 2.060(2) Å] (Table 2). The shortest M^{II}–N bonds are again found for the most electronegative analogues (**8**, Ni^{II}) with larger values found for early metal derivatives (**5**, Mn^{II}). The N1–M1–N1A bond angles are linear while the N1–M1–O bond angles range from 85.90(6) to 94.10(6)° and 87.9(1) to 92.1(1)° for **5** and **8**, respectively (Table 3) [20g,45]. The W(1)···W1A and M2···M2A contacts are 8.644(3) and 6.590(3) Å for **5** while comparatively smaller values [8.394(3) and 6.382(3) Å] are found for **8**.

3.3. Crystallographic studies: two-dimensional sheets

Crystals of **6** and **10** crystallize in the monoclinic $P2_1/n$ and $P2_1/c$ space groups, respectively (Table 1). The neutral, corrugated two-dimensional sheets contain [*cis*-M^{II}(DMF)$_4$(μ-NC)$_2$]$^{2+}$, [*trans*-M^{II}(DMF)$_4$(μ-NC)$_2$]$^{2+}$, and three-connected [M^V(CN)$_5$(μ-CN)$_3$]$^{3-}$ units that are linked via cyanides into 12-membered rings in a 4:2:6 ratio (Fig. 2), respectively; the asymmetric unit and 12-membered ring fragments present in **6** are illustrated in Figs. 3 and 4. The 12-membered rings are the basic building units of the corrugated two-dimensional sheets (Fig. 3), with each offset by *ca.* 5 Å and linked via shared [*trans*-M^{II}-(μ-NC)$_2$(DMF)$_4$]$^{2+}$ units to adjacent [M^V(CN)$_8$]$^{3-}$ centers. The ruffled sheets are separated by *ca.* 6.8 [Mn···Mn] and 7.0 Å [Fe···Fe] for **6** and **10**, respectively, and are comparable to those reported (*ca.* 7.0 Å) for structurally related two-dimensional $Mn_3^{II}Mo_2^V$ lattices (**11**) [20g,45]. The ring dimensions are *ca.* 10 [W1A···W1E] × 18 Å [W1A···W1B] and 11 [W1···W1A] × 18 [W1···W1E] for **6** and **10**, respectively, being slightly smaller than reported for 2-D $Mn_3^{II}Mo_2^V$ (**11**) analogues (*ca.* 9 × 24 Å) [45].

The W–C bond distances and C–W–C angles are within the ranges expected for octacyanometalate networks (Table 2). The W–C bonds vary from 2.158(3) to 2.179(3) Å for **6** and 2.155(6) and 2.177(6) Å for **10**, while the C–W–C bond angles range from 70.60(9) to 148.13(9)° and 70.5(2) to 148.0(2)° for **6** and **10**, respectively; again the tungsten centers have distorted square antiprismatic coordination geometries. The terminal and bridging cyanide W–C–N angles are also nearly linear ranging from 176.2(2) to 179.1(2) and 174.9(4) to 179.7(5)° for **6** and **10**, respectively (Table 3).

In **6** and **10** the two-dimensional lattices consist of 12-membered rings that are composed of [*trans*-M^{II}(μ-NC)$_2$(DMF)$_4$]$^{2+}$ and [*cis*-M^{II}(μ-NC)$_2$(DMF)$_4$]$^{2+}$ units. The [*trans*-M^{II}(μ-NC)$_2$(DMF)$_4$]$^{2+}$ units have M–N and M–O bond distances that are slightly longer than those seen in the [*cis*-M^{II}(μ-NC)$_2$(DMF)$_4$]$^{2+}$ fragments (Table 2). The M–N and M–O bond distances in the [*trans*-M^{II}(μ-NC)$_2$(DMF)$_4$]$^{2+}$ fragments are 2.232(2) and 2.154(4) Å, while those for the [*cis*-M^{II}(μ-NC)$_2$(DMF)$_4$]$^{2+}$ units are slightly shorter, being 2.217(2) and 2.170(4) Å for **6** and **10**, respectively; similar bond distance trends are observed in **5**, **7**, and **8**.

The N–M–N and O–M–O bond angles also exhibit structure-dependent changes depending on their location within the 2-D sheets (Table 3). For [*trans*-M^{II}-(DMF)$_4$]$^{2+}$ fragments, the symmetry related N–M–N angles are 180°, while the O–M–O angles range from 87.4(3) to 180° for **6** and 88.6(1) to 180° for **10**. In comparison, the N–M–N and O–M–O angles for the [*cis*-M^{II}-(μ-NC)$_2$(DMF)$_4$]$^{2+}$ fragments range between 88.57(7) and 169.66(6)° and 86.8(1) and 173.2(2)° for **6** and **10**, respectively, being close to those seen for structurally related $Mn_3^{II}Mo_2^V$ (**11**) lattices [20g,45].

3.4. Crystallographic studies of 9

Crystals of **9** are in the monoclinic $P2_1/c$ space group and crystallize as trimetallic salts of [Fe^{II}(DMF)$_6$]$_2$-[W^{IV}(CN)$_8$] stoichiometry (Table 1). The W–C bond distances range from 2.167(3) to 2.181(3) Å while the C–W–C bond angles are between 70.9(2) and 145.3(1)°; the W–C–N angles are nearly linear, ranging from 178.7(3) to 179.3(3)° (Fig. 5). The Fe–O lengths are all slightly different, ranging from 1.975(2) [Fe1–O1A] to 2.196(2) Å [Fe2–O1F], while the O–Fe–O bond angles are nearly octahedral, ranging from 87.49(9) to 93.05(9)° [O1D–Fe2–O1F and O1A–Fe1–O1B]. The [Fe^{II}(DMF)$_6$]$^{2+}$ and [W^{IV}(CN)$_8$]$^{4-}$ ions are well-separated and are not related by rotational symmetry; the Fe1···Fe2, Fe1···W1, and Fe2···W1 contacts are 9.66(2), 7.16(3), and 8.88(3) Å, respectively (see Fig. 6).

3.5. Magnetic studies

Magnetic studies of suggest that the magnetic exchange interactions present in the Mn^{II}(μ-NC)W^V units of **5** and **6** are antiferromagnetic [20g]. The room temperature χT values for **5** and **6** [13.73 and 14.15 emu K mol^{-1}] are close to the spin-only value (13.88 emu K mol^{-1}) expected for a 3:2 ratio of non-interacting W^V ($S = 1/2$; $g = 2$) and Mn^{II} ($S = 1/2$; $g = 2$) centers. The sign of the local exchange interactions can often be predicted from the shape of the χT versus T curve. A shallow minimum is often found when short-range antiferromagnetic correlations compensate spins [49] and such minima are observed at *ca.* 75 and 200 K for **5** and **6**, respectively. At lower temperatures the χT product monotonically increases reaching maximum values of 24.82 and 151.2 emu K mol^{-1} at 3.7 and 10.0 K, with χT again decreasing towards minimum values of 23.41 and 99.7 emu K mol^{-1} at 1.8 and 5 K, for **5** and **6**, respectively. Fitting of the χ^{-1} versus T data (at $H_{dc} = 1$ kG) with the Curie–Weiss expression affords negative Weiss constants (−0.66 K for **5** and −4.78 K for **6**) ver-

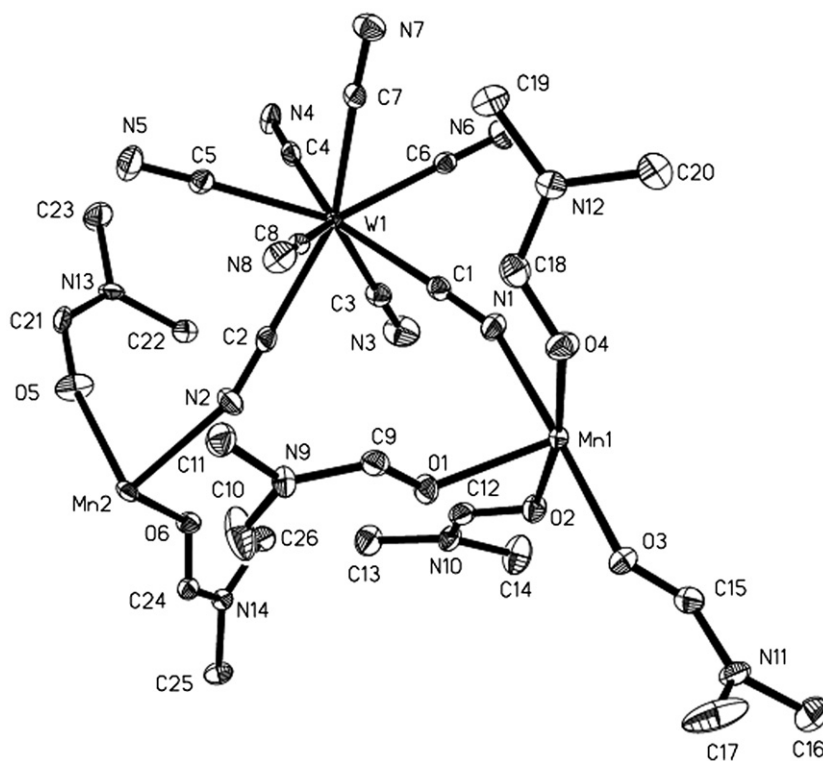Fig. 3. Asymmetric unit of **6**. Thermal ellipsoids are at the 50% level and all hydrogen atoms are removed for clarity.
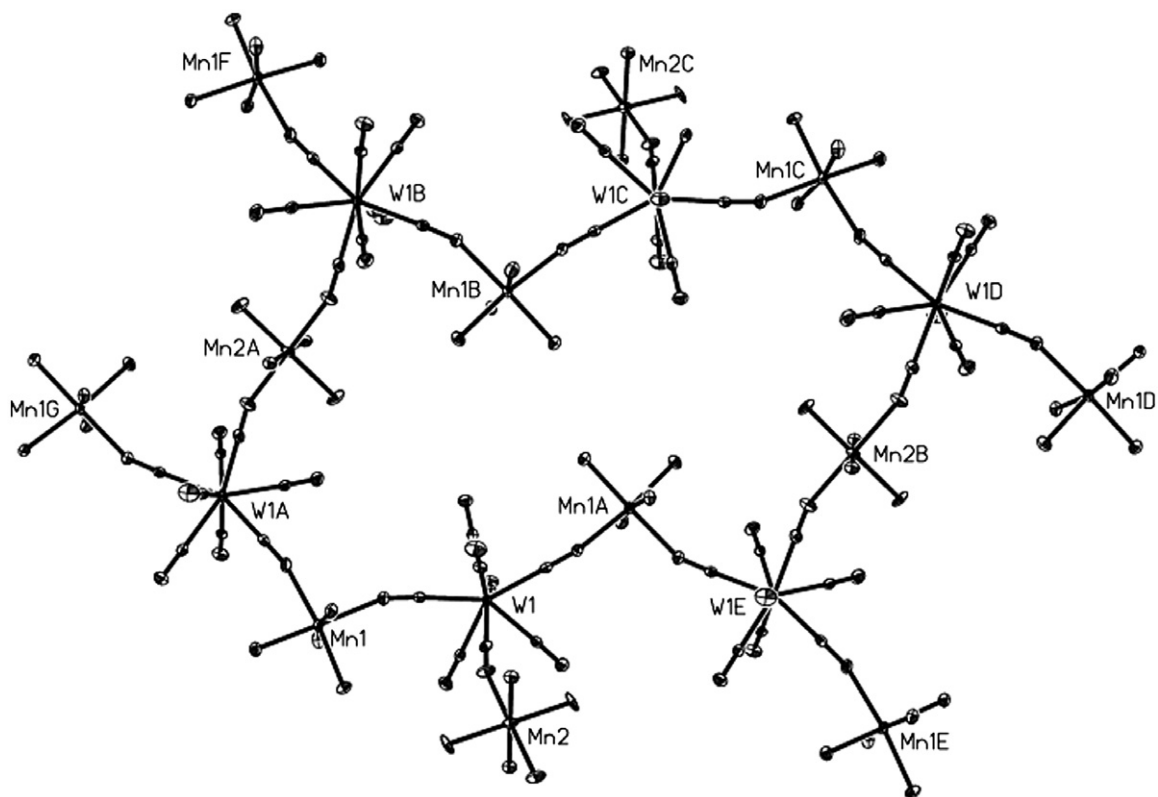

Fig. 4. X-ray structure of **6** illustrating the 12-membered rings present. Thermal ellipsoids are at the 50% level, DMF ligands are truncated, and all hydrogen atoms are removed for clarity.
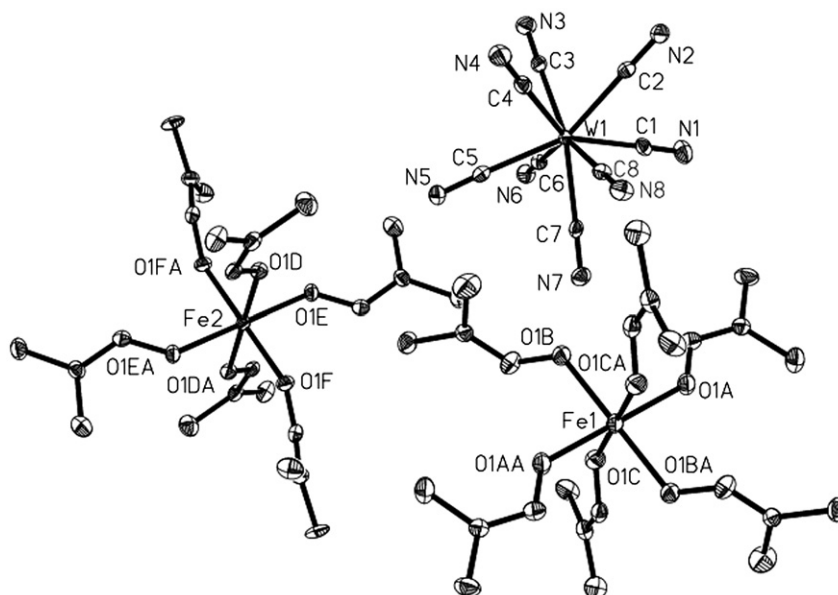
Fig. 5. X-ray structure of **9**. Thermal ellipsoids are at the 50% probability level and all hydrogen atoms are removed for clarity.
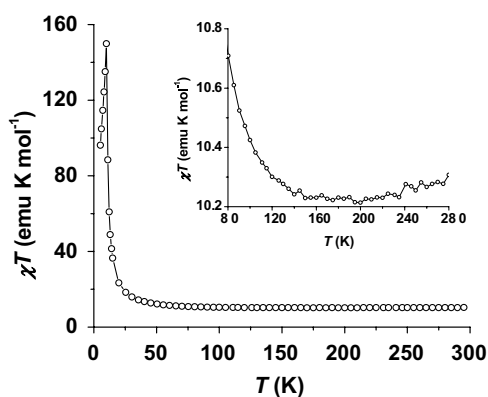

Fig. 6. Temperature dependence of χT for **6** at $H_{dc} = 1$ kG.
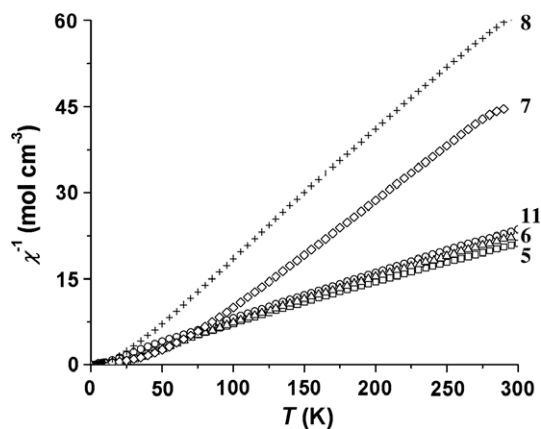
Fig. 7. Temperature dependence of the reciprocal susceptibility for **5–8** and **11** at $H_{dc} = 1$ kG.

Fig. 8. Temperature dependence of zero-field-cooled (□) and field-cooled (○) magnetization for **6** ($H_{dc} = 2$ G).

ifying that local antiferromagnetic interactions are present. As judged from the divergence of the zero-field-cooled and field-cooled magnetization curves ($H_{dc} = 2$ G) we conclude that $T_N = 8$ K for **6** (Fig. 8), while **5** does not appear to exhibit long-range magnetic ordering above 1.8 K.

The field dependence of the magnetization at 2 K further indicates that the Mn^{II} and W^V ions in **5** and **6** engage in antiferromagnetic exchange interactions. The experimental saturation magnetization values ($H_{dc} = 70$ kG) for **5** and **6** are 72.3 and 73.4 kG cm^3 mol^{-1} and are close to the expected value of 72.61 kG cm^3 mol^{-1} assuming that $g = 2$. Both **5** and **6** exhibit closed hysteresis loops and small coercive fields (Fig. 9) consistent with the presence of isotropic metal ions.

For **7** and **8** cyanide-mediated superexchange within the $Ni^{II}(\mu\text{-NC})M^V$ units is expected to be ferromagnetic (Ni^{II}, $S = 1$) assuming that the magnetic orbitals are orthogonal and that Goodenough–Kanamori rules are applicable [1–8h,50]. Using crushed single crystals of **7** and **8** the room-
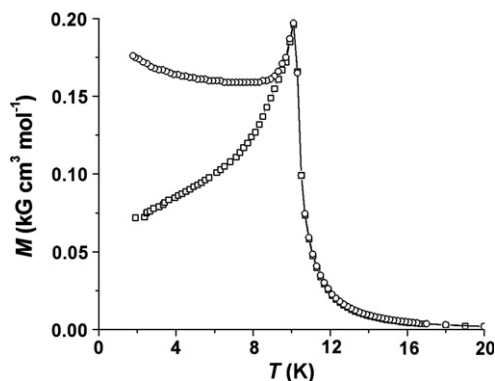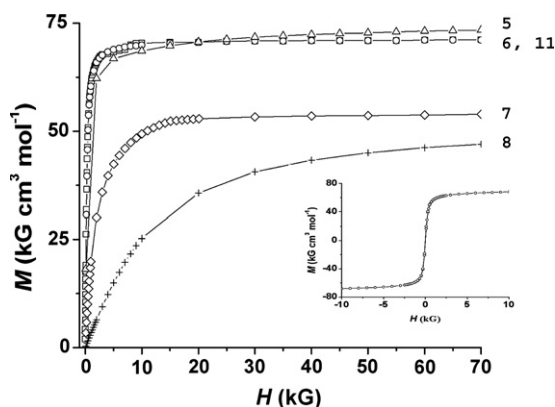
Fig. 9. Field dependence of the magnetization for **5–8** and **11** at 2 K. Inset: Hysteresis of **6** at 2 K.
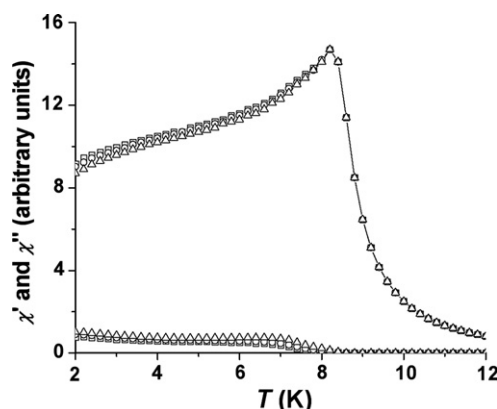

Fig. 10. Temperature dependence of the real (χ', top) and imaginary components (χ'', bottom) of the ac susceptibility for **6** ($H_{dc} = 0$ Oe; $H_{ac} = 3$ Oe) at 1 (○), 10 (△), and 100 (□) Hz.

temperature χT values [6.43 and 5.32 emu K mol^{-1}] are near the expected (5.92 emu K mol^{-1}, $g_{Ni} = 2.2$ assumed) value for a 3:2 ratio of non-interacting Ni^{II} ($S = 1$) and M^V ($S = 1/2$; Mo, W) spin centers. The temperature dependence of the χT product ($H_{dc} = 1$ kG) suggests that the Ni^{II} and M^V (Mo^V and W^V) centers undergo short-range ferromagnetic exchange interactions, with χT increasing as a function of decreasing temperature, reaching maximum values [36.72 emu K mol^{-1} for **7** and 50.03 emu K mol^{-1} for **8**] at 19 and 3.8 K for **7** and **8**, respectively. Fitting the χ^{-1} versus T data via the Curie–Weiss expression affords positive Weiss constants (47.56 K for **7** and 11.87 K for **8**) verifying that local ferromagnetic interactions are present (Fig. 7) [20g].

The field dependence of the magnetization data suggests that the cyanide-bridged transition metal centers present in **7** and **8** are ferromagnetically coupled at 1.8 K and large H_{dc} (Fig. 9). Assuming that $g = 2$ the expected saturation magnetization value is 48.03 kG cm^3 mol^{-1} and is between the experimental values found for **7** and **8** [53.9 and 47.0 kG cm^3 mol^{-1}]. Lastly the field dependence of the magnetization indicates that **7** and **8** exhibit closed hysteresis loops with negligible coercive fields at 1.8 K [20g].

ac susceptibility measurements suggest that χ'' is frequency-dependent for **6** despite the presence of isotropic metal ions, while **5**, **7**, and **8** exhibit no frequency-dependent behavior ($H_{dc} = 0$ G; $H_{ac} = 3.5$ G). Using freshly-prepared, crushed crystals of **5**, we find that χ'' is invariant with respect to changing frequency, in stark contrast to reports claiming that structurally-related 1-D [Mn^{II}(b-py)$_2$]$_3$[W^V(CN)$_8$]$_2$ lattices exhibit frequency-dependent χ'' maxima [23,24]. However for samples of **5** (ca. 2 weeks) unsymmetrical and broad frequency-dependent maxima (Fig. 10) are observed in plots of χ'' versus T, that appear to increase in intensity with respect to time and increasing temperature; the frequency-dependent peaks in χ'' are qualitatively similar to those found for Tang's 1-D chains, **6**, and a recently reported 2-D [Mn^{II}(DMF)$_4$]$_3$[Mo^V(CN)$_8$]$_2$ lattice (**11**) [23,24,45]. The unsymmetrical χ'' peak is

suggestive of multiple relaxation processes, the presence of multiple magnetic phases, and/or that **5**, **6**, and [Mn^{II}(DMF)$_4$]$_3$[Mo^V(CN)$_8$]$_2$ are unstable under the conditions of the ac susceptibility measurements [20g]. For freshly prepared samples of **5**, **7**, and **8** we tentatively propose that they exhibit incipient magnetic ordering in the presence of large H_{dc} fields.

3.6. Chemical and thermal stability of networks

Heating crystalline samples of **5** and **6** decreases the intensity of the DMF $\nu_{C=O}$ stretching absorption while the energies and intensities of the ν_{CN} absorptions remain unchanged. We previously reported that heated samples of **11** afford additional magnetic phases ($T_N \sim 21$ K), that are not due to linkage isomerism [2c,51], but rather desolvation followed by aggregation [20h,45]. Unfortunately all attempts to structurally characterize the microcrystalline and amorphous solids precipitated from hot reaction mixtures containing crystals of **5–8** or **11** have consistently met with failure.

Furthermore, the isolation of one- and two-dimensional phases (**5** and **6**) from essentially the same reaction conditions (at or near 300 K) suggests that the M^{II}(μ-NC)M^V linkages can be ruptured to form a variety of aggregated products under relatively mild conditions. At lower reaction temperatures (20 °C) and short reaction times a 1-D chain of squares lattice (**5**) is obtained, while longer reaction times and higher temperatures (28 °C) appear to afford 2-D phases (**6**); to date only 2-D lattices have been obtained when using **1** as a starting material. In the absence of counterions (HNBu$_3^+$ and OTs$^-$) crystals of **5** do not transform into **6** when stored at room temperature (28 °C) in DMF over 3 weeks, in addition to small quantities of DMF-insoluble amorphous precipitates. However, in the presence of counterions (DMF solution, 28 °C) **5** transforms into **6** over a period of weeks, as judged via indexing several crystals removed from the reaction mixture. In addition, wet DMF mixtures of **1** or **2** in the pres-

ence of manganese(II) tosylate exclusively affords 2-D phases in addition to amorphous precipitates. Apparently wet DMF accelerates the transformation of **5** into **6** and attempts to insert other metal centers (e.g. Fe^{II}, Co^{II}, Ni^{II}) into the lattice affords intractable precipitates. To date only Mn^{II} analogues appear to undergo slow one- to two-dimensional phase changes. We propose that formation **5** precedes **6**, being highly dependent on the quantity of water and counterions present. In the presence of counterions we presume that for **5**, labilization of coordinated DMF and rupture of the $Mn^{II}(\mu\text{-}NC)M^V$ linkages afford soluble species that undergo aggregation, gradually transforming the chains into the two-dimensional corrugated sheets found in **6** [46e].

4. Conclusions

We have described the synthesis, structural, infrared, and magnetic characterization of a trimetallic salt and several one- and two-dimensional networks derived from octacyanometalate(V) centers. Coordinated DMF appears to limit the number of cyano linkages formed and the dimensionality of the resulting lattices. The one-dimensional chains appear to exhibit short-range magnetic interactions but no spontaneous magnetic ordering above 1.8 K. Surprisingly, conversion of one- to two-dimensional crystalline phases in the presence of counterions occurs in solution, while heating of crystalline samples introduces an additional magnetic phases without linkage isomerism. Two-dimensional phases containing Mn^{II} centers appear to be the sole product when wet DMF is used as a reaction solvent. The experimental evidence suggests that coordinated DMF ligands are labile and the $M^{II}(\mu\text{-}NC)M^V$ linkages are susceptible to fragmentation.

Acknowledgements

Appendix A. Supplementary material

CCDC 621773, 621774, 621775, 621776 and 621777 contain the supplementary crystallographic data for this paper. These data can be obtained free of charge via http://www.ccdc.cam.ac.uk/conts/retrieving.html, or from the Cambridge Crystallographic Data Centre, 12 Union Road, Cambridge CB2 1EZ, UK; fax: (+44) 1223-336-033; or e-mail: deposit@ccdc.cam.ac.uk. Supplementary data associated with this article can be found, in the online version, at doi:10.1016/j.poly.2007.01.049.

References

[1] W.R. Entley, G.S. Girolami, Science 268 (1995) 397.
[2] (a) M. Verdaguer, A. Bleuzen, V. Marvaud, J. Vaissermann, M. Seuleiman, C. Desplanches, A. Scuiller, C. Train, R. Garde, G. Gelly, C. Lomenech, I. Rosenman, P. Veillet, C. Cartier, F. Villain, Coord. Chem. Rev. 190–192 (1999) 1023;
(b) K.R. Dunbar, R.A. Heintz, Prog. Inorg. Chem. 45 (1997) 283;
(c) A.G. Sharpe, The Chemistry of Cyano Complexes of the Transition Metals, Academic Press, New York, 1976.
[3] S. Ferlay, T. Mallah, R. Ouahès, P. Veillet, M. Verdaguer, Nature 378 (1995) 701.
[4] S.M. Holmes, G.S. Girolami, J. Am. Chem. Soc. 121 (1999) 5593.
[5] Ø. Hatlevik, W.E. Buschmann, J. Zhang, J.L. Manson, J.S. Miller, Adv. Mater. 11 (1999) 914.
[6] D. Gatteschi, O. Kahn, J.S. Miller, F. Palacio (Eds.), Magnetic Molecular Materials, Kluwer, Dordrecht, 1991.
[7] C.P. Landee, D. Melville, J.S. Miller, in: D. Gatteschi, O. Kahn, J.S. Miller, F. Palacio (Eds.), Magnetic Molecular Materials, NATO ASI Series E, vol. 198, Plenum, New York, 1991.
[8] (a) L.M.C. Beltran, J.R. Long, Acc. Chem. Res. 38 (2005) 325;
(b) J.J. Sokol, A.G. Hee, J.R. Long, J. Am. Chem. Soc. 124 (2002) 7656;
(c) C.P. Berlinguette, D. Vaughn, C. Cañada-Vilalta, J.R. Galán-Mascarós, K.R. Dunbar, Angew. Chem., Int. Ed. 42 (2003) 1523;
(d) A.V. Palii, S.M. Ostrovsky, S.I. Klokishner, B.S. Tsukerblat, C.P. Berlinguette, K.R. Dunbar, J.R. Galán-Mascarós, J. Am. Chem. Soc. 126 (2004) 16860;
(e) E.J. Schelter, A.V. Prosvirin, K.R. Dunbar, J. Am. Chem. Soc. 126 (2004) 15004;
(f) S. Wang, J.-L. Zuo, H.-C. Zhou, H.J. Choi, Y. Ke, J.R. Long, X.-Z. You, Angew Chem., Int. Ed. 43 (2004) 5940;
(g) K.R. Dunbar, E.J. Schelter, A.V. Palii, S.M. Ostrovsky, V.Y. Mirovitski, J.M. Hudson, M.A. Omary, S.I. Klokishner, B.S. Tsukerblat, J. Phys. Chem. A 107 (2003) 11102;
(h) E.J. Schelter, A.V. Prosvirin, W.M. Reiff, K.R. Dunbar, Angew. Chem., Int. Ed. 42 (2004) 4912;
(i) H. Miyasaka, H. Takahashi, T. Madanbashi, K.-I. Sugiura, R. Clérac, H. Nojiri, Inorg. Chem. 44 (2005) 5969;
(j) M. Ferbinteanu, H. Miyasaka, W. Wernsdorfer, K. Nakata, K.-I. Sugiura, M. Yamashita, C. Coulon, R. Clérac, J. Am. Chem. Soc. 127 (2005) 3090;
(k) D. Li, S. Parkin, G. Wang, G.T. Yee, A.V. Prosvirin, S.M. Holmes, Inorg. Chem. 44 (2005) 4903;
(l) D. Li, R. Clérac, S. Parkin, G. Wang, G.T. Yee, S.M. Holmes, Inorg. Chem. 45 (2006) 5251;
(m) D. Li, R. Clérac, S. Parkin, G. Wang, G.T. Yee, S.M. Holmes, Inorg. Chem. 45 (2006) 7569;
(n) D. Li, S. Parkin, G. Wang, G.T. Yee, R. Clérac, W. Wernsdorfer, S.M. Holmes, J. Am. Chem. Soc. 128 (2006) 4214;
(o) K. Park, S.M. Holmes, Phys. Rev. B (in press);
(p) D. Li, S. Parkin, R. Clérac, G. Wang, G.T. Yee, S.M. Holmes, Eur. J. Inorg. Chem., doi:10.1002/ejic.200600819;
(q) D. Li, C. Ruschman, S. Parkin, R. Clérac, S.M. Holmes, Chem. Commun. 4036 (2006);
(r) D. Li, S. Parkin, G. Wang, G.T. Yee, S.M. Holmes, Inorg. Chem. 45 (2006) 1951.
[9] (a) L.M. Toma, R. Lescouëzec, F. Lloret, M. Julve, M. Verdaguer, Inorg. Chem. 41 (2002) 818;
(b) R. Lescouëzec, J. Vaissermann, C. Ruiz-Pérez, F. Lloret, R. Carrasco, M. Julve, M. Verdaguer, Y. Dromzee, D. Gatteschi, W.

Wernsdorfer, Angew. Chem., Int. Ed. 42 (2003) 1483;
(c) S. Wang, J.-L. Zho, S. Gao, Y. Song, H.-C. Zhou, Y.-Z. Zhang, X.-Z. You, J. Am. Chem. Soc. 126 (2004) 8900.

[10] (a) O. Sato, Acc. Chem. Res. 36 (2003) 692, and references therein;
(b) Y. Arimoto, S. Ohkoshi, Z.J. Zhong, H. Seino, Y. Mizobe, K. Hashimoto, J. Am. Chem. Soc. 125 (2003) 9240;
(c) T. Yokoyama, K. Okamoto, T. Ohta, S.-I. Ohkoshi, K. Hashimoto, Phys. Rev. 65B (2001) 1;
(d) S. Ohkoshi, K. Hashimoto, J. Am. Chem. Soc. 121 (1999) 10591;
(e) O. Sato, T. Iyoda, A. Fujishima, K. Hashimoto, Science 272 (1996) 704;
(f) O. Sato, Y. Einaga, T. Iyoda, A. Fujishima, K. Hashimoto, Inorg. Chem. 38 (1999) 4405;
(g) N. Shimamoto, S.-I. Ohkoshi, O. Sato, K. Hashimoto, Inorg. Chem. 41 (2002) 678;
(h) A. Bleuzen, C. Lomenech, V. Escax, F. Villain, F. Varret, C. Cartier dit Moulin, M. Verdaguer, J. Am. Chem. Soc. 122 (2000) 6648;
(i) C. Cartier dit Moulin, F. Villain, A. Bleuzen, M. Arrio, P. Sainctavit, C. Lomenech, V. Escax, F. Baudelet, E. Dartyge, M. Verdaguer, J. Am. Chem. Soc. 122 (2000) 6653;
(j) S. Ohkoshi, S. Yorozu, O. Sato, T. Iyoda, A. Fujishima, K. Hashimoto, Appl. Phys. Lett. 70 (1977) 1040;
(k) S. Ohkoshi, Y. Einaga, A. Fujishima, K. Hashimoto, J. Electroanal. Chem. 473 (1999) 245;
(l) S. Ohkoshi, M. Mizuno, G. Hung, K. Hashimoto, J. Phys. Chem. 40 (2000) 9365;
(m) Z.-Z. Gu, O. Sato, T. Iyoda, K. Hashimoto, A. Fujishima, J. Phys. Chem. 100 (1996) 18289;
(n) Z.-Z. Gu, O. Sato, T. Iyoda, K. Hashimoto, A. Fujishima, Chem. Mater. 9 (1997) 1092;
(o) S.-I. Ohkoshi, K. Hashimoto, J. Photochem. Photobiol. C: Photochem. Rev. 2 (2001) 71;
(p) S. Ohkoshi, N. Machida, J. Zhong, Z.J. Hashimoto, Synth. Met. 122 (2001) 523;
(q) G. Rombaut, M. Verelst, S. Golhen, L. Ouahab, C. Mathonière, O. Kahn, Inorg. Chem. 40 (2001) 1151.

[11] R. Billing, A.J. Vogler, J. Photochem. Photobiol. A: Chem. 103 (1997) 239.

[12] S.I. Ali, K. Majid, Thermochim. Acta 317 (1998) 141.

[13] A.K. Sra, M. Andruh, O. Kahn, S. Golhen, L. Ouahab, J.V. Yakhmi, Angew. Chem., Int. Ed. 38 (1999) 2606.

[14] G. Rombaut, S. Golhen, L. Ouahab, C. Mathonière, O. Kahn, J. Chem. Soc., Dalton Trans. 3609 (2000).

[15] (a) A. Yuan, J. Zou, B. Li, Z. Zha, C. Duan, Y. Liu, Z. Xu, S. Keizer, Chem. Commun. 1297 (2000);
(b) M. Ohba, N. Fukita, H. Ōkawa, J. Chem. Soc., Dalton Trans. 1733 (1997);
(c) H. Kou, W. Bu, D. Liao, Z. Jiang, S. Yan, Y. Fan, G. Wang, J. Chem. Soc., Dalton Trans. 4161 (1998);
(d) M. Ohba, N. Usuki, N. Fukita, H. Ōkawa, Inorg. Chem. 37 (1998) 3349;
(e) N. Fukita, M. Ohba, H. Ōkawa, K. Matsuda, H. Iwamura, Inorg. Chem. 37 (1998) 842;
(f) S. Zhang, D. Fu, W. Sun, Z. Hu, K. Yu, W. Tang, Inorg. Chem. 39 (2000) 1142;
(g) N. Usuki, M. Yamada, M. Ohba, H. Ōkawa, J. Solid St. Chem. 159 (2001) 328;
(h) M. Ohba, H. Ōkawa, N. Fukita, Y. Mashimoto, J. Am. Chem. Soc. 119 (1997) 1011;
(i) F. Thétiot, S. Triki, J.S. Pala, New J. Chem. 26 (2002) 196;
(j) H.-Z. Kou, J.-K. Tang, D.-Z. Liao, S. Gao, P. Cheng, Z.-H. Jiang, S.-P. Yan, G.-L. Wang, B. Chansou, J. Tuchagues, Inorg. Chem. 40 (2001) 4839.

[16] (a) W.R. Bucknall, W. Wardlaw, J. Chem. Soc. 2981 (1927);
(b) W.U. Malik, S.I. Ali, Bull. Chem. Soc. Jpn. 1306 (1961);
(c) W.U. Malik, S.I. Ali, Bull. Chem. Soc. Jpn. 1310 (1961);
(d) G.F. McKnight, G.P. Haight, Inorg. Chem. 12 (1973) 3007.

[17] J.M. Herrera, D. Armentano, G. de Munno, F. Lloret, M. Julve, M. Verdaguer, New J. Chem. 27 (2003) 128.

[18] (a) J.M. Herrera, A. Bleuzen, Y. Dromzée, M. Julve, F. Lloret, M. Verdaguer, Inorg. Chem. 42 (2003) 7052;
(b) S. Willemin, J. Larionova, R. Clérac, B. Donnadieu, B. Henner, X.F. Le Goff, C. Guérin, Eur. J. Inorg. Chem. 1866 (2003).

[19] A.K. Sra, G. Rombaut, F. Lahitête, S. Golhen, L. Ouahab, C. Mathonière, J.V. Yakhmi, O. Kahn, New J. Chem. 24 (2000) 871.

[20] (a) Y. Arimoto, S. Ohkoshi, Z.J. Zhong, H. Sieno, Y. Mizobe, K. Hashimoto, J. Am. Chem. Soc. 125 (2003) 9240;
(b) A. Bleuzen, C. Lomenech, V. Escax, F. Villain, F. Varret, C. Cartier dit Moulin, M. Verdaguer, J. Am. Chem. Soc. 122 (2000) 6648;
(c) D. Li, L. Zheng, X. Wang, J. Huang, S. Gao, W. Tang, Chem. Mater. 15 (2003) 2094;
(d) D. Li, T. Okamura, W. Sun, N. Ueyama, W. Tang, Cryst. Struct. Commun. C58 (2002) m280;
(e) D. Li, D. Yang, S. Li, W. Tang, Inorg. Chem. Commun. 5 (2002) 791;
(f) R. Podgajny, Y. Dromzée, K. Kruczała, B. Sieklucka, Polyhedron 20 (2001) 685;
(g) F. Chang, H.-L. Sun, H.-Z. Kou, S. Gao, Inorg. Chem. Commun. 5 (2002) 660;
(h) W. Meske, D.Z. Babel, Anorg. Allg. Chem. 625 (1999) 51;
(i) A.K. Sra, G. Rombaut, F. Lahitête, S. Golhen, L. Ouahab, C. Mathonière, J.V. Yakhmi, O. Kahn, New J. Chem. 24 (2000) 871;
(j) R. Billing, A.J. Vogler, J. Photochem. Photobiol. A: Chem. 103 (1997) 239;
(k) S.I. Ali, K. Majid, Thermochim. Acta 317 (1998) 141;
(l) A.K. Sra, M. Andruh, O. Kahn, S. Golhen, L. Ouahab, J.V. Yakhmi, Angew. Chem., Int. Ed. 38 (1999) 2606;
(m) G. Rombaut, S. Golhen, L. Ouahab, C. Mathonière, O. Kahn, J. Chem. Soc., Dalton Trans. (2000) 3609;
(n) R. Kania, K. Lewinski, B. Sieklucka, Dalton Trans. (2003) 1033;
(o) J.M. Herrera, V. Marvaud, M. Verdaguer, J. Marrot, M. Kalisz, C. Mathonière, Angew. Chem., Int. Ed. 43 (2004) 5467;
(p) J.R. Withers, C. Ruschman, P. Bojang, S. Parkin, S.M. Holmes, Inorg. Chem. 44 (2005) 352;
(q) S.-I. Ohkoshi, Y. Einaga, A. Fujishima, K. Hashimoto, J. Electroanal. Chem. 473 (1999) 245;
(r) S.-I. Ohkoshi, M. Mizuno, G. Hung, K. Hashimoto, J. Phys. Chem. 40 (2000) 9365;
(s) Z.-Z. Gu, O. Sato, T. Iyoda, K. Hashimoto, A. Fujishima, J. Phys. Chem. 100 (1996) 18289;
(t) Z.-Z. Gu, O. Sato, T. Iyoda, K. Hashimoto, A. Fujishima, Chem. Mater. 9 (1997) 1092;
(u) S.-I. Ohkoshi, K. Hashimoto, J. Photochem. Photobiol. C: Photochem. Rev. 2 (2001) 71;
(v) S.-I. Ohkoshi, N. Machida, Z.J. Zhong, K. Hasimoto, Synth. Met. 122 (2001) 523;
(w) G. Rombaut, M. Verelst, S. Golhen, L. Ouahab, C. Mathonière, O. Kahn, Inorg. Chem. 40 (2001) 1151;
(x) J.R. Withers, C. Ruschman, S. Parkin, S.M. Holmes, Polyhedron 24 (2005) 1845.

[21] (a) S. Willemin, J. Larionova, R. Clérac, B. Donnadieu, B. Henner, X.F. Le Goff, C. Guérin, Eur. J. Inorg. Chem. (2003) 1866;
(b) B. Sieklucka, J. Szklarzewicz, T.J. Kemp, W. Errington, Inorg. Chem. 39 (2000) 5156;
(c) J. Larionova, R. Clérac, B. Donnadieu, S. Willemin, C. Guérin, Cryst. Growth Des. 3 (2003) 267.

[22] (a) Y. Song, P. Zhang, X.-M. Ren, X.-F. Shen, Y.-Z. Li, X.-Z. You, J. Am. Chem. Soc. 127 (2005) 3708;
(b) Z.J. Zhong, H. Seino, Y. Mizobe, M. Hidai, A. Fujishima, S. Ohkoshi, K. Hashimoto, J. Am. Chem. Soc. 122 (2000) 2952;
(c) J. Larionova, M. Gross, H.A. Pilkington, H. Stoeckli-Evans, H.U. Güdel, S. Decurtins, Angew. Chem., Int. Ed. 39 (2000) 1605;
(d) F. Bonadio, M. Gross, H. Stoeckli-Evans, S. Decurtins, Inorg. Chem. 41 (2002) 5891;

(e) Z.J. Zhong, H. Seino, Y. Mizobe, M. Hidai, M. Verdaguer, S. Ohkoshi, K. Hashimoto, Inorg. Chem. 39 (2000) 5095;
(f) Unpublished results;
(g) See the Supporting Section;
(h) E. Ruiz, G. Rajaraman, S. Alvarez, B. Gillon, J. Stride, R. Clérac, J. Larionova, S. Decurtins, Angew. Chem., Int. Ed. 44 (2005) 2711.

[23] D. Li, L. Zheng, Y. Zhang, J. Huang, S. Gao, W. Tang, Inorg. Chem. 42 (2003) 6123.

[24] D. Li, S. Gao, L. Zhong, W. Tang, J. Chem. Soc., Dalton Trans. 2805 (2002).

[25] S.M. Holmes, S.G. McKinley, G.S. Girolami, P.S. Szalay, K.R. Dunbar, Inorg. Synth. 33 (2002) 91.

[26] J.G. Leipoldt, L.D. Bok, P.J. Cilliers, Z. Anorg. Allg. Chem. 409 (1974) 343.

[27] N.H. Furman, C.O. Miller, P.G. Arvan, L.F. Audrieth, Inorg. Synth. 3 (1950) 160.

[28] L.D. Bok, J.D. Leipoldt, S.S. Basson, Z. Anorg. Allg. Chem. 415 (1975) 81.

[29] R.L. Carlin, Magnetochemistry, Springer-Verlag, New York, 1986.

[30] O. Kahn, Molecular Magnetism, VCH, New York, 1993.

[31] Z. Otwinowski, W. Minor, Methods Enzymol. 276 (1997) 307.

[32] (a) G.M. Sheldrick, SADABS – An Empirical Absorption Correction Program. Bruker Analytical X-Ray Systems; Madison, Wisconsin, 1996;
(b) G.M. Sheldrick, SHELX-97. Programs for Crystal Structure Solution and Refinement, University of Gottingen, Germany, 1997.

[33] International Tables for Crystallography vol. C: Kluwer Academic Publishers, Dordrecht, The Netherlands, 1992.

[34] (a) M. Bogdanov, R. Grybos, A. Samotus, K. Bogolitsyn, Trans. Met. Chem. Dordrecht 18 (1993) 599;
(b) C.R. Dennis, S.S. Basson, J.G. Leipoldt, Polyhedron 2 (1983) 1357;
(c) D. Li, S. Gao, L. Zheng, K. Yu, W. Tang, New. J. Chem. 26 (2002) 1190;
(d) A. Marchaj, A. Plesinski, Z. Stasicka, Rocz. Chem. 50 (1976) 1239.

[35] (a) W.L. Waltz, A.W. Adamson, P.D. Fleischauer, J. Am. Chem. Soc. 89 (1967) 3923;
(b) K.R. Butter, T.J. Kemp, B. Sieklucka, A. Samotus, J. Chem. Soc., Dalton Trans. 1217 (1986);
(c) S. Zofia, B. Hanna, Rocz. Chem. 48 (1974) 389;
(d) S.I. Zofia, Rocz. Chem. 47 (1973) 1993;
(e) G.W. Gray, J.T. Spence, Inorg. Chem. 10 (1971) 2751;
(f) Unpublished results.

[36] K. Nakamoto, Infrared and Raman Spectra of Inorganic and Coordination Compounds, Part B, Fifth ed., Wiley, New York, 1997, pp. 54–58 and 105–116.

[37] (a) Y. Arimoto, S. Ohkoshi, Z.J. Zhong, H. Seino, Y. Mizobe, K. Hashimoto, Chem. Lett. 832 (2002);
(b) Y. Song, S. Ohkoshi, Y. Arimoto, H. Seino, Y. Mizobe, K. Hashimoto, Inorg. Chem. 42 (2003) 1848;
(c) T. Korzeniak, R. Podgajny, N.W. Alcock, K. Lewiński, M. Bałanda, T. Wasiutyński, B. Sieklucka, Polyhedron 22 (2003) 2183;
(d) D. Li, L. Zheng, X. Wang, J. Huang, S. Gao, W. Tang, Chem. Mater. 15 (2003) 2094;
(e) D. Li, S. Gao, L. Zheng, W. Sun, T. Okamura, N. Ueyama, W. Tang, New J. Chem. 26 (2002) 485.

[38] (a) B. Sieklucka, J. Szklarzewicz, T.J. Kemp, W. Errington, Inorg. Chem. 39 (2000) 5156;
(b) T. Kashiwagi, S.-I. Ohkoshi, H. Seino, Y. Mizobe, K. Hashimoto, J. Am. Chem. Soc. 126 (2004) 5024.

[39] T.V. Long, G.A. Vernon, J. Am. Chem. Soc. 93 (1971) 1919.

[40] K.O. Hartman, F.A. Miller, Spectrochim. Acta 24A (1968) 669.

[41] E.G. Brame, F.A. Johnson, E.M. Larsen, V.W. Meloche, J. Inorg. Nucl. Chem. 2 (1958) 99.

[42] (a) R. Podgajny, B. Sieklucka, W. Łasocha, J. Chem. Soc., Dalton Trans. 1799 (2000);
(b) W.P. Griffith, J. Chem. Soc., Dalton Trans. 2489 (1975).

[43] W. Meske, D. Babel, Z. Anorg. Allg. Chem. 625 (1999) 51.

[44] F. Chang, H.-L. Sun, H.-Z. Kou, S. Gao, Inorg. Chem. Commun. 5 (2002) 660.

[45] J.R. Withers, D. Li, J. Triplet, C. Ruschman, S. Parkin, G. Wang, G.T. Yee, S.M. Holmes, Inorg. Chem. 45 (2006) 4307.

[46] (a) C.A. Bignozzi, R. Argazzi, J.R. Schoonover, K.C. Gordon, R.B. Dyer, F. Scandola, Inorg. Chem. 31 (1992) 5260;
(b) M.A. Watzky, J.F. Endicott, X. Song, Y. Lei, A. Mccatangay, Inorg. Chem. 35 (1996) 3463;
(c) K.F. Purcell, S.M. Yeh, J.S. Eck, Inorg. Chem. 16 (1977) 1708;
(d) M.Y. Darensbourg, H.L.C. Barros, Inorg. Chem. 18 (1979) 3286;
(e) M.J. Scott, R.H. Holm, J. Am. Chem. Soc. 116 (1994) 11357;
(f) H. Vahrenkamp, A. Geiss, G.N. Richardson, J. Chem. Soc., Dalton Trans. 3643 (1997);
(g) B.S. Lim, R.H. Holm, Inorg. Chem. 37 (1998) 4898;
(h) G.N. Richardson, U. Brand, H. Vahrenkamp, Inorg. Chem. 38 (1999) 3070;
(i) A. Geiss, H. Vahrenkamp, Eur. J. Inorg. Chem. 1793 (1999);
(j) A. Geiss, H. Vahrenkamp, Inorg. Chem. 39 (2000) 4029;
(k) R. Podgajny, C. Desplanches, B. Sieklucka, R. Sessoli, V. Villar, C. Paulsen, W. Wernsdorfer, Y. Dromzée, M. Verdaguer, Inorg. Chem. 41 (2002) 1323;
(l) C.A. Bignozzi, F. Scandola, Inorg. Chem. 23 (1984) 1540;
(m) K.F. Purcell, J. Am. Chem. Soc. 89 (1967) 247;
(n) K.F. Purcell, Inorg. Chem. 89 (1967) 6139.

[47] P.M. Kiernan, W.P. Griffith, J. Chem. Soc., Dalton Trans. 2489 (1975).

[48] (a) E. Colacio, J.M. Domínguez-Vera, F. Lloret, A. Rodriguez, H. Stoeckli-Evans, Inorg. Chem. 42 (2003) 6962;
(b) D.W. Knoeppel, J. Liu, F.A. Meyers, S.G. Shore, Inorg. Chem. 37 (1998) 4828;
(c) D.W. Knoeppel, S.G. Shore, Inorg. Chem. 35 (1996) 1747;
(d) J.A. Smith, J.-R. Galán-Mascarós, R. Clérac, J.-S. Sun, X. Quyang, K.R. Dunbar, Polyhedron 20 (2001) 1727;
(e) C.P. Berlinguette, J.A. Smith, J.-R. Galán-Mascarós, K.R. Dunbar, CR Acad. Sci., Ser. IIc: Chim. 5 (2002) 665;
(f) C.P. Berlinguette, J.-R. Galán-Mascarós, K.R. Dunbar, Inorg. Chem. 42 (2003) 3416.

[49] (a) A. Caneschi, D. Gatteschi, A.L. Lirzin, J. Mater. Chem. 4 (1994) 319;
(b) A. Caneschi, D. Gatteschi, J.P. Renard, P. Rey, R. Sessoli, J. Am. Chem. Soc. 111 (1989) 785;
(c) A. Caneschi, D. Gatteschi, P. Rey, R. Sessoli, Inorg. Chem. 27 (1988) 1756;
(d) H.O. Stumpf, L. Ouahab, Y. Pey, D. Grandjean, O. Kahn, Science 261 (1993) 447;
(e) M. Hitzfield, P. Ziemann, W. Buckel, H. Claus, Phys. Rev. B 29 (1984) 5023.

[50] (a) J.B. Goodenough, J. Appl. Phys. 39 (1968) 403;
(b) J.P. Goodenough, Phys. Rev. 164 (1967) 785;
(c) J.B. Goodenough, Magnetism and the Chemical Bond, Interscience, New York, 1953;
(d) J.B. Goodenough, Phys. Rev. 100 (1955) 564;
(e) J.B. Goodenough, J. Phys. Chem. Solids 6 (1958) 287;
(f) J. Manamori, J. Phys. Chem. Solids 10 (1959) 87.

[51] (a) D.B. Brown, D.F. Shriver, Inorg. Chem. 8 (1969) 37;
(b) E. Reguera, J.F. Bertrán, L. Nuñez, Polyhedron 13 (1994) 1619;
(c) D.B. Brown, D.F. Shriver, L.H. Schwartz, Inorg. Chem. 7 (1968) 77;
(d) J.E. House, J.C. Bailar Jr., Inorg. Chem. 8 (1969) 672;
(e) D.B. Brown, D.F. Shriver, S.E. Anderson, Inorg. Chem. 4 (1965) 725.